SUPPORTING INFORMATION

Charge-compensated *nido*-carborane derivatives in the synthesis of iron(II) bis(dicarbollide) complexes

Marina Yu. Stogniy,[a,b] Sergey A. Anufriev,[a] Ekaterina V. Bogdanova,[a,b] Nadezhda A. Gorodetskaya,[a,b] Alexei A. Anisimov,[a] Kyrill Yu. Suponitsky,[a,c] Ivan D. Grishin,[d] and Igor B. Sivaev [a,e]

[a] *A.N. Nesmeyanov Institute of Organoelement Compounds, Russian Academy of Sciences, Moscow, Russia.*
[b] *M.V. Lomonosov Institute of Fine Chemical Technology, MIREA - Russian Technological University, Moscow, Russia*
[c] *G.V. Plekhanov Russian University of Economics, Moscow, Russia*
[d] *Lobachevsky State University of Nizhny Novgorod, Nizhny Novgorod, Russia*
[e] *Faculty of Chemistry, National Research University Higher School of Economics (HSE University), Moscow, Russia*

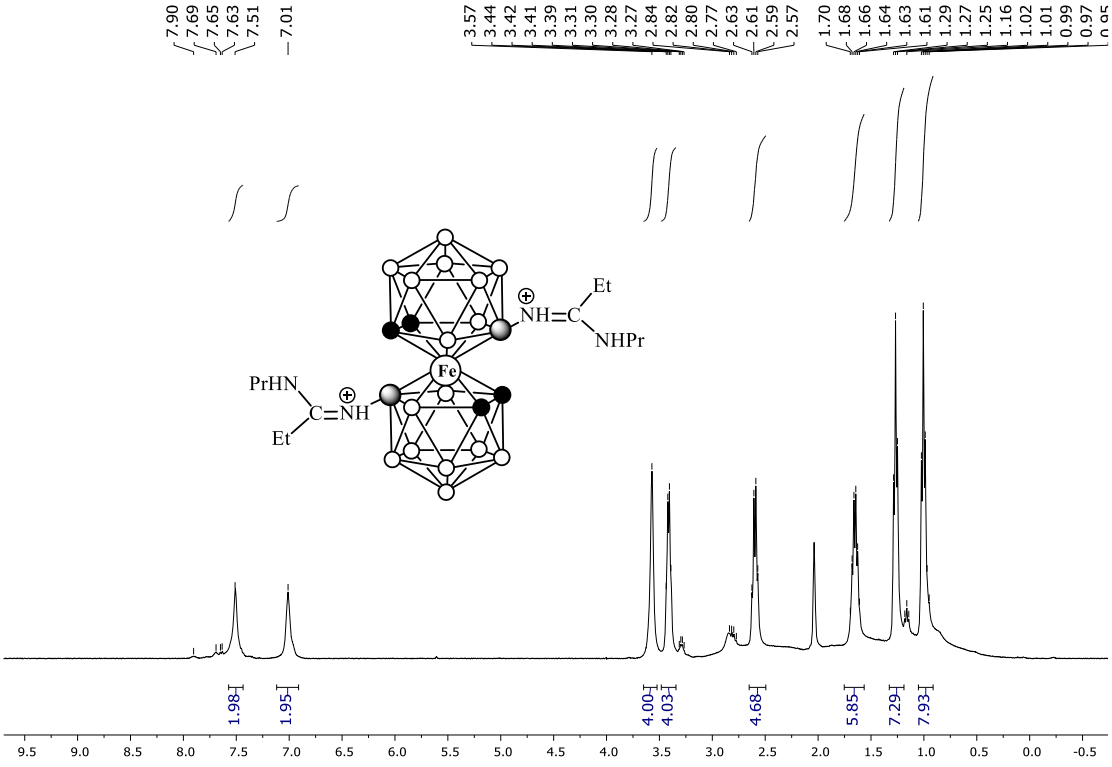

Fig. S1. ^{1}H NMR spectrum of compound **6** (acetone-d_6).

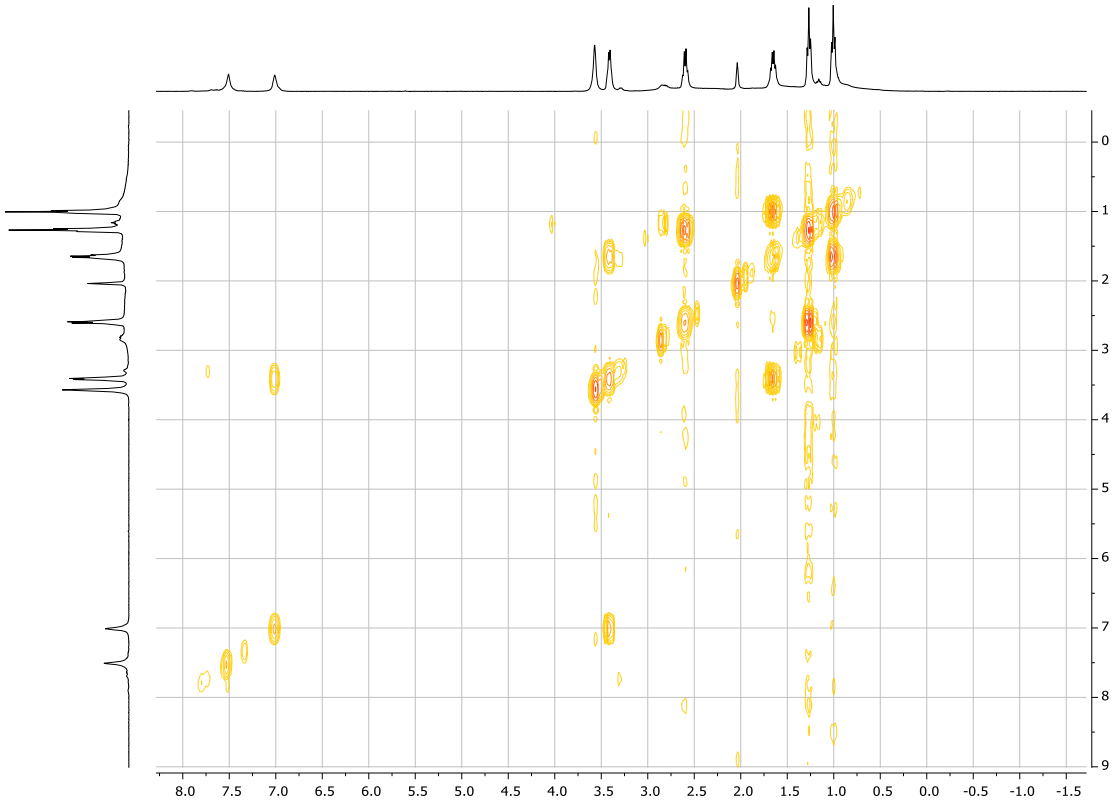

Fig. S2. ^{1}H-^{1}H COSY NMR spectrum of compound **6** (acetone-d_6).

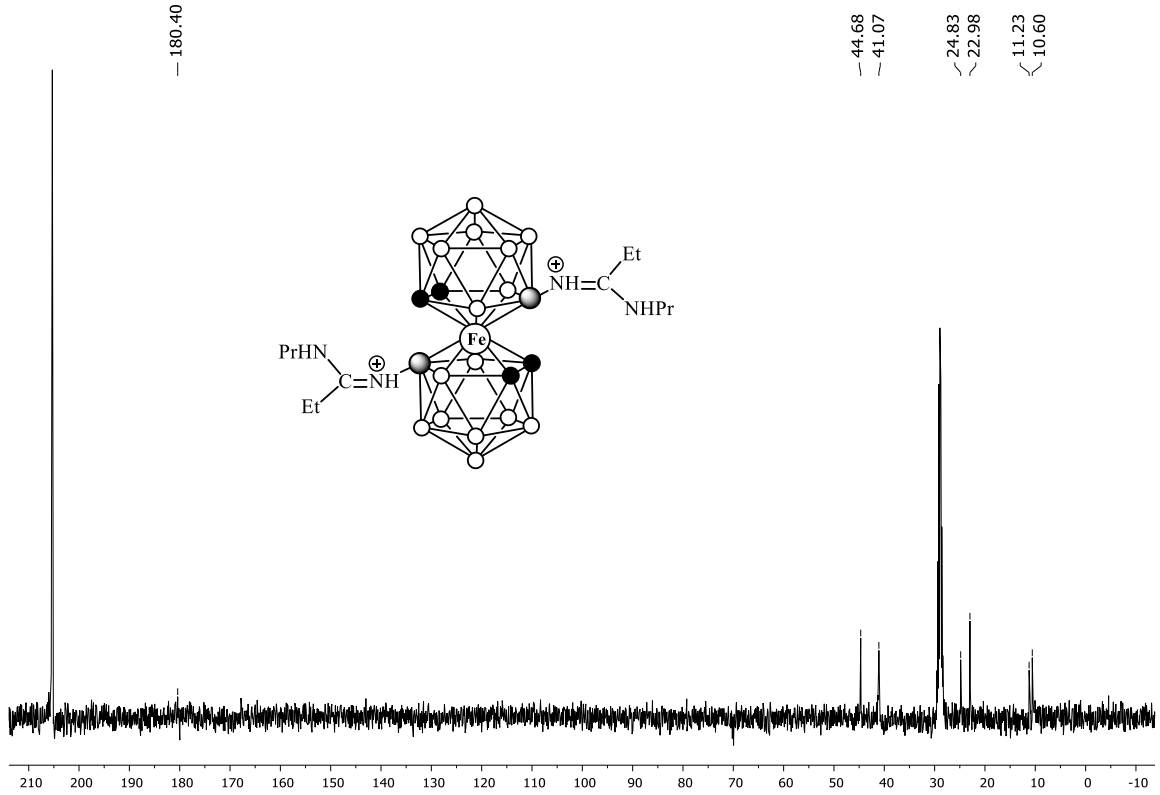

Fig. S3. ^{13}C NMR spectrum of compound **6** (acetone-d_6).

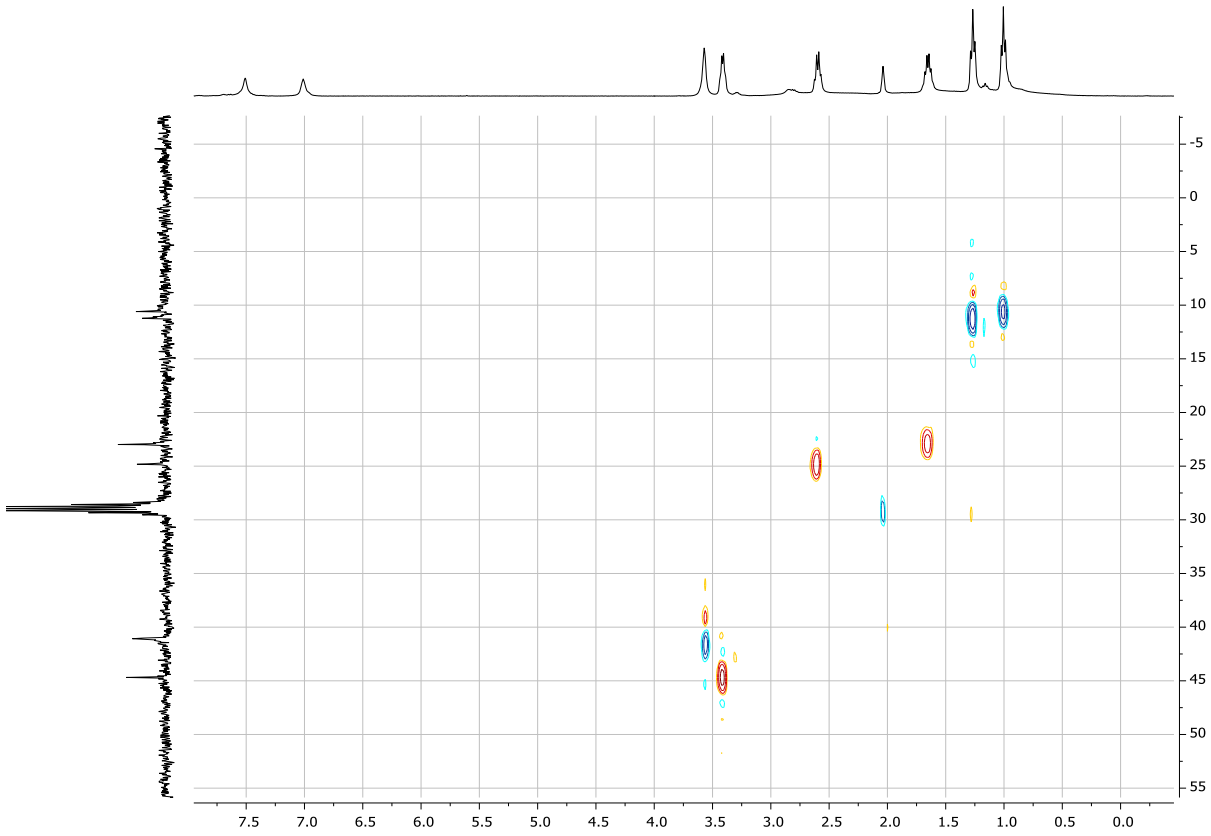

Fig. S4. ^{1}H-^{13}C HSQC NMR spectrum of compound **6** (acetone-d_6).

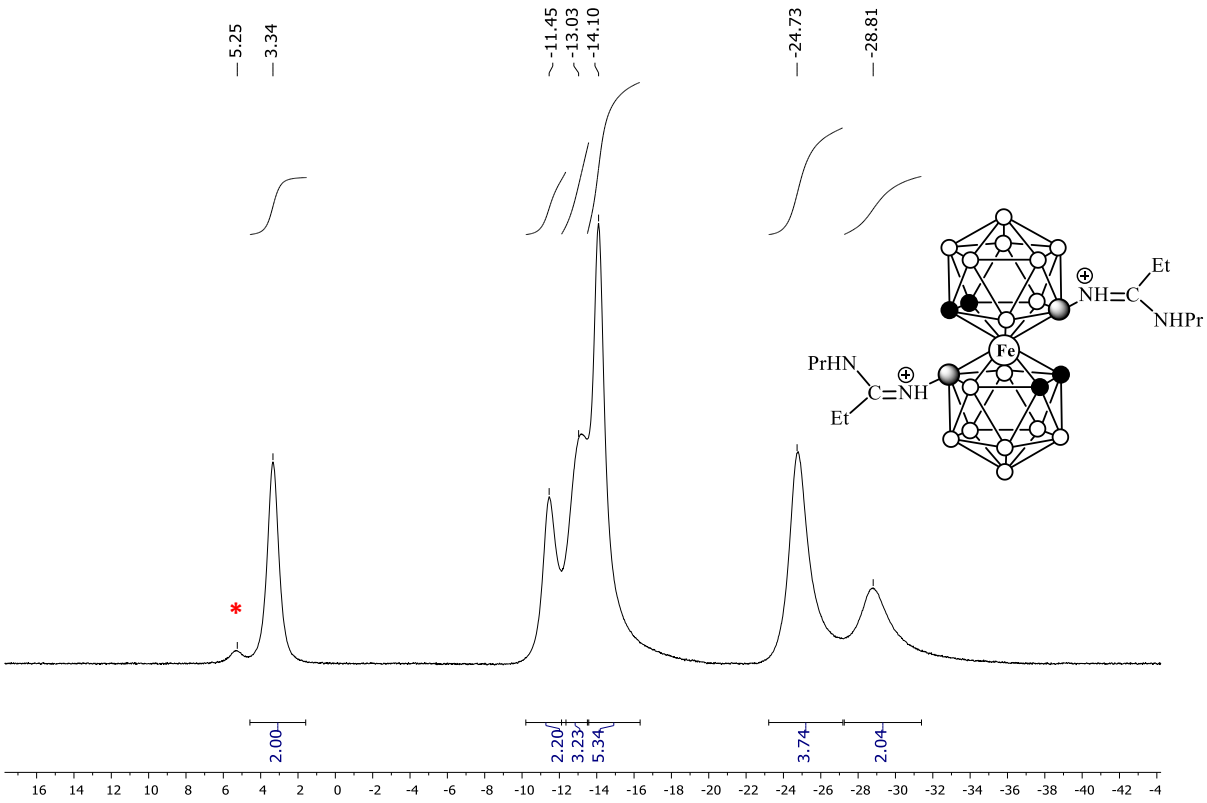

* minor isomers signal

Fig. S5. $^{11}B\{^{1}H\}$ NMR spectrum of compound **6** (acetone-d_6).

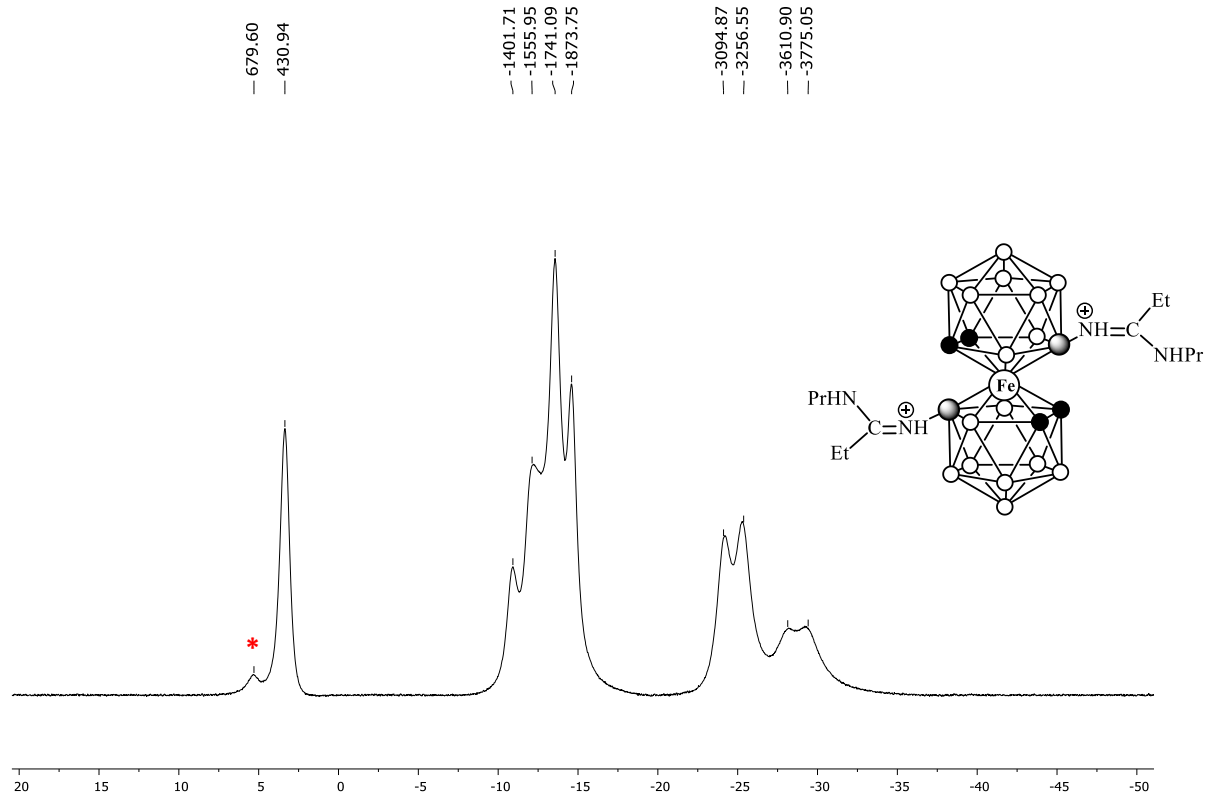

* minor isomers signal

Fig. S6. ^{11}B NMR spectrum of compound **6** (acetone-d_6).

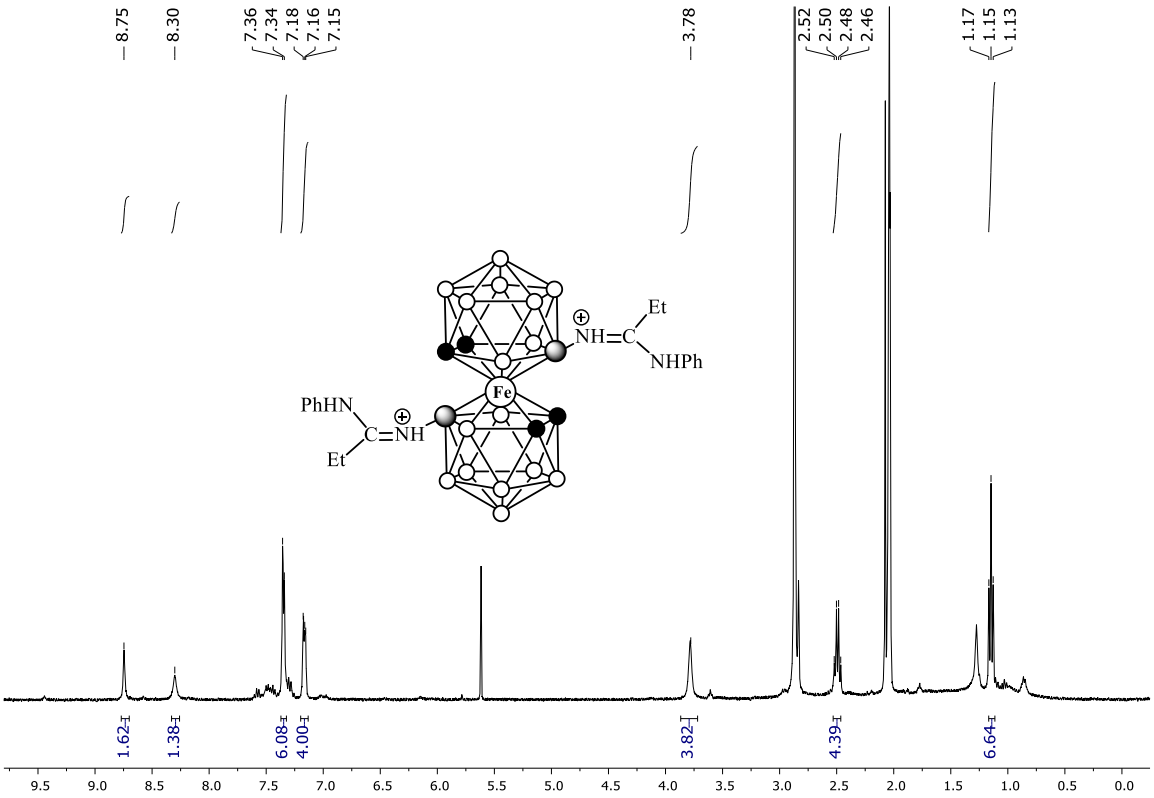

Fig. S7. ^{1}H NMR spectrum of compound **7** (acetone-d_6).

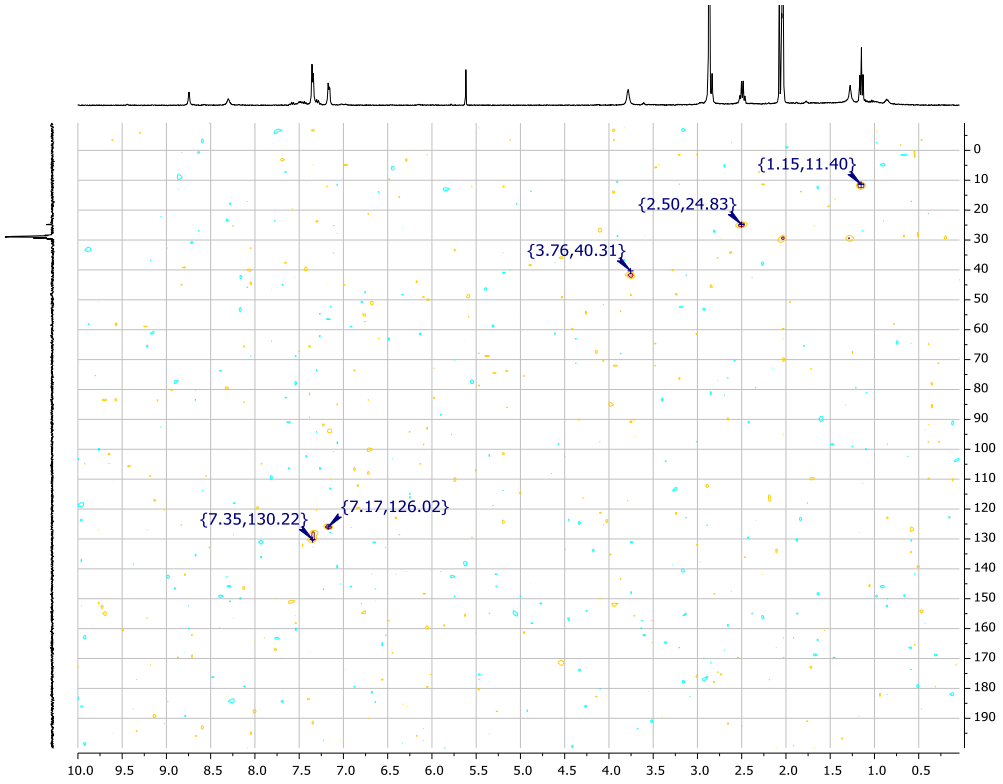

Fig. S8. ^{1}H-^{13}C HSQC NMR spectrum of compound **7** (acetone-d_6).

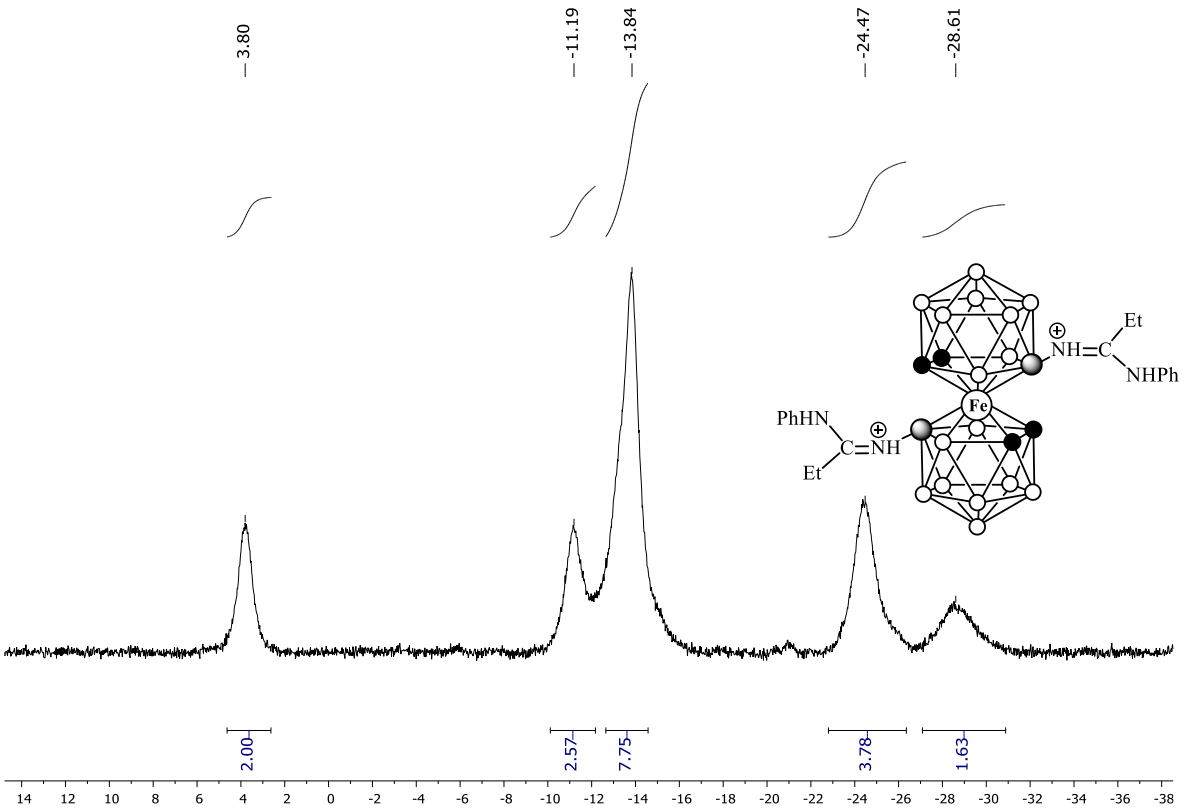

Fig. S9. $^{11}B\{^{1}H\}$ NMR spectrum of compound **7** (acetone-d_6).

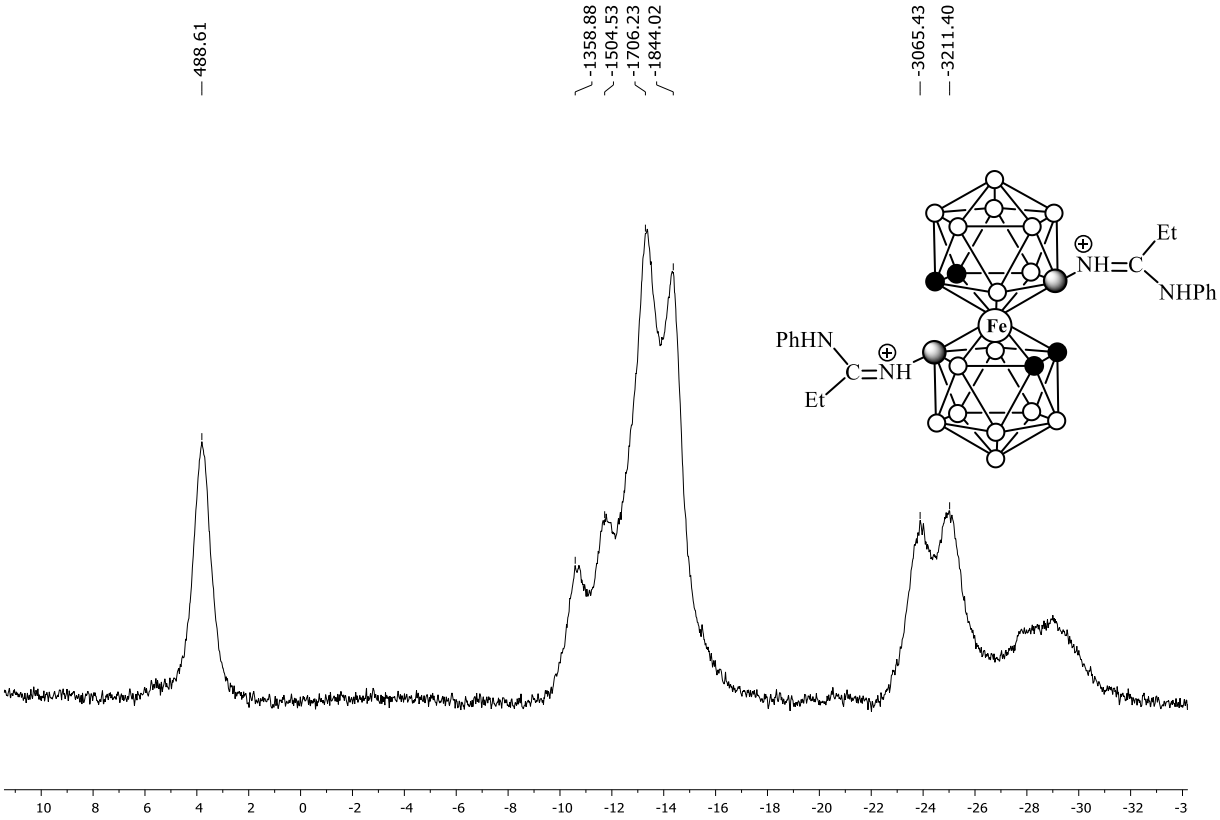

Fig. S10. ^{11}B NMR spectrum of compound **7** (acetone-d_6).

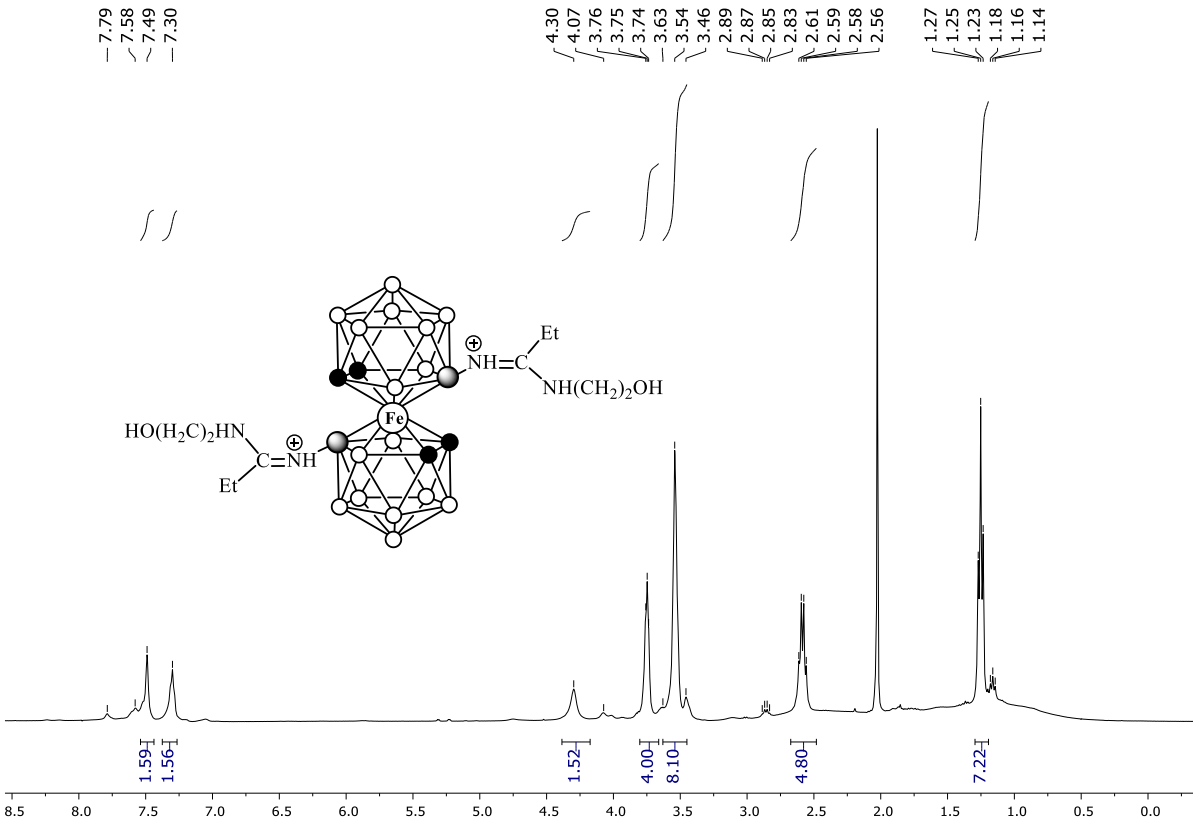

Fig. S11. ^{1}H NMR spectrum of compound **8** (acetone-d_6).

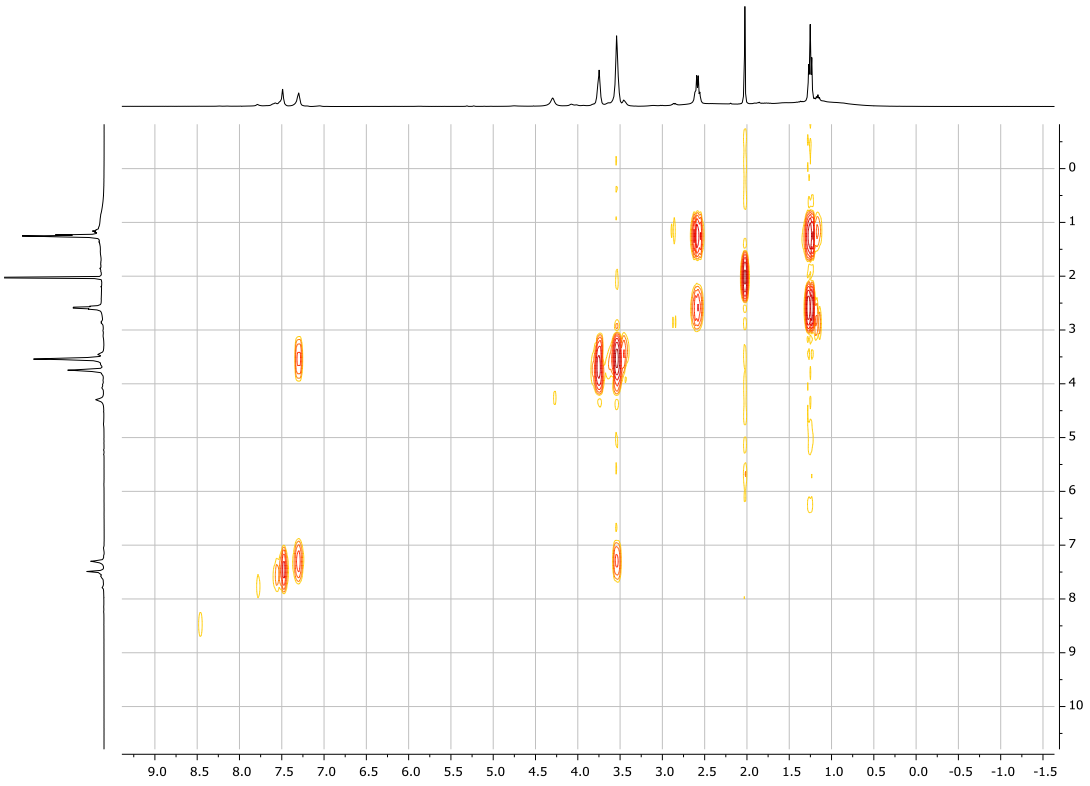

Fig. S12. ^{1}H-^{1}H COSY NMR spectrum of compound **8** (acetone-d_6).

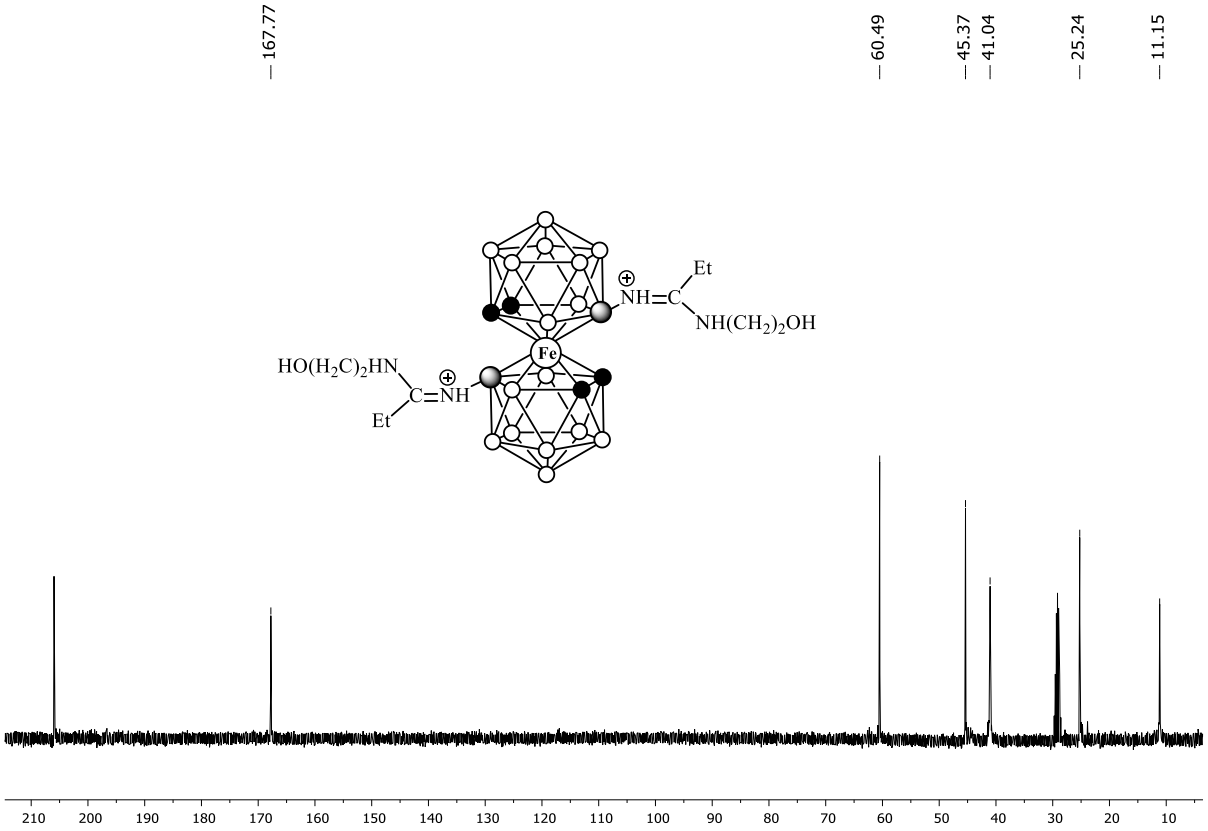

Fig. S13. ^{13}C NMR spectrum of compound **8** (acetone-d_6).

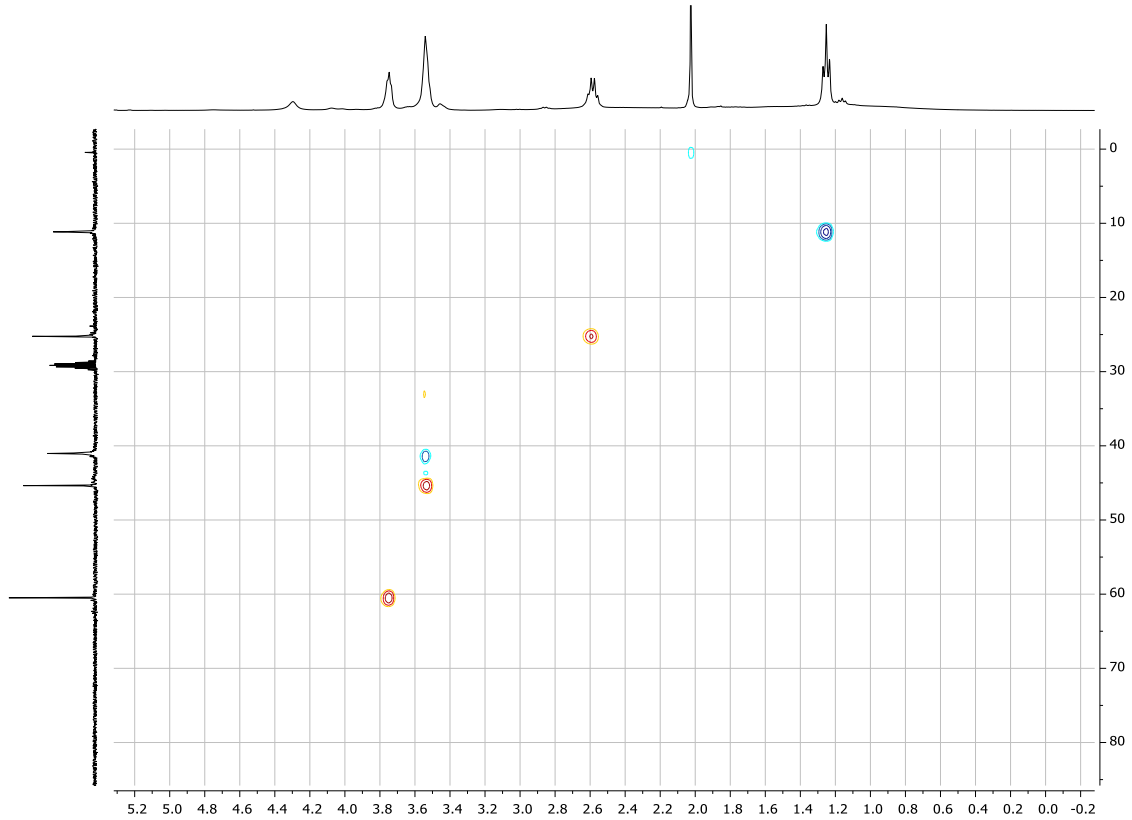

Fig. S14. ^{1}H-^{13}C HSQC NMR spectrum of compound **8** (acetone-d_6).

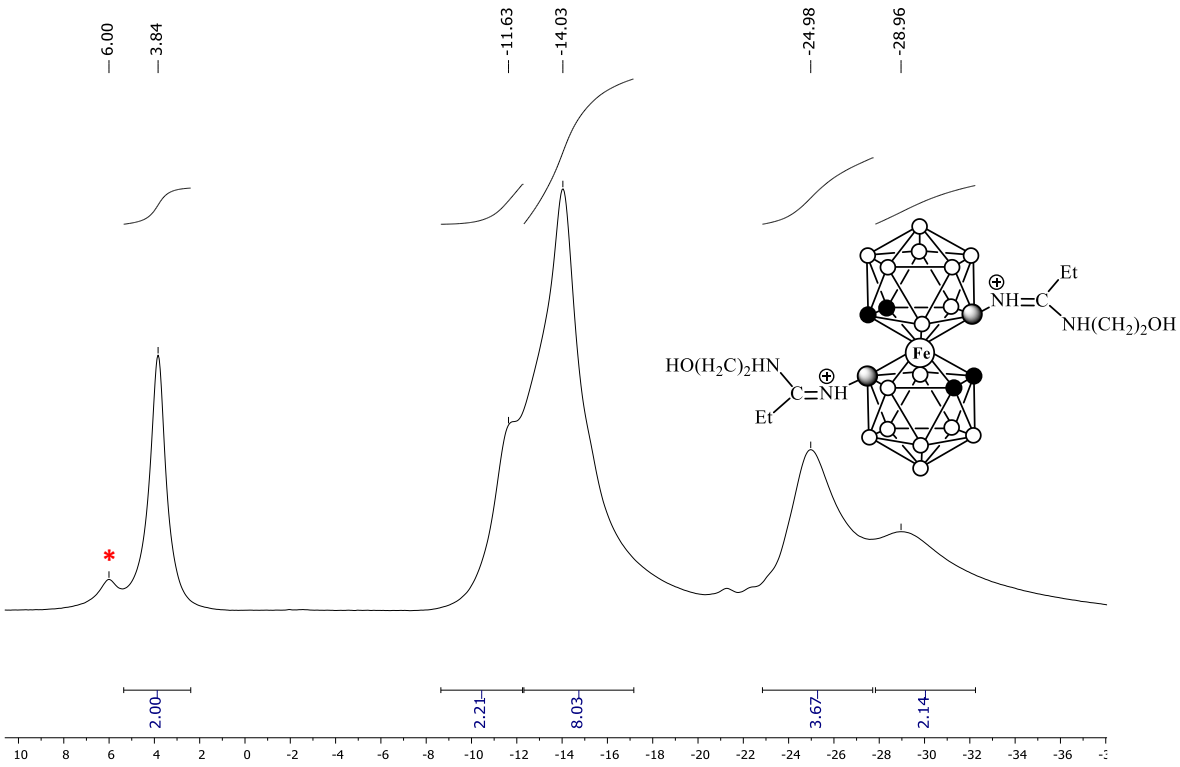

* minor isomers signal

Fig. S15. $^{11}B\{^{1}H\}$ NMR spectrum of compound **8** (acetone-d_6).

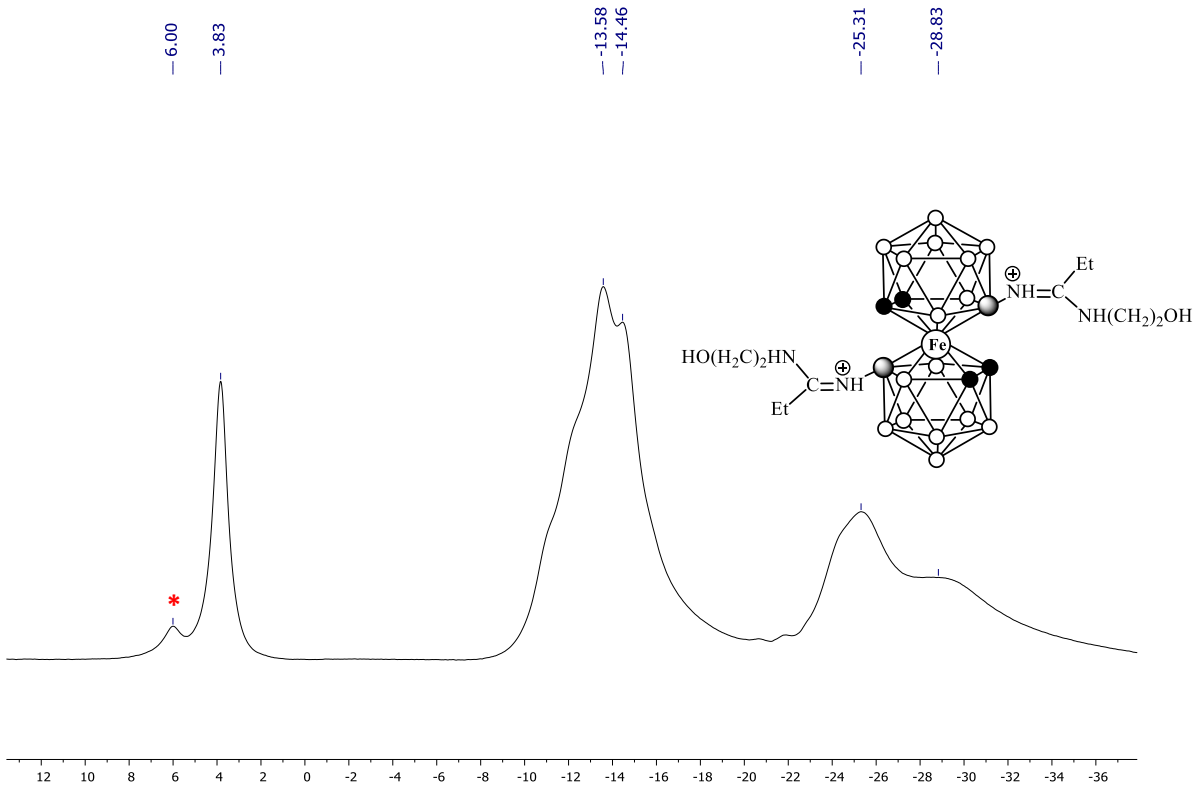

* minor isomers signal

Fig. S16. ^{11}B NMR spectrum of compound **8** (acetone-d_6).

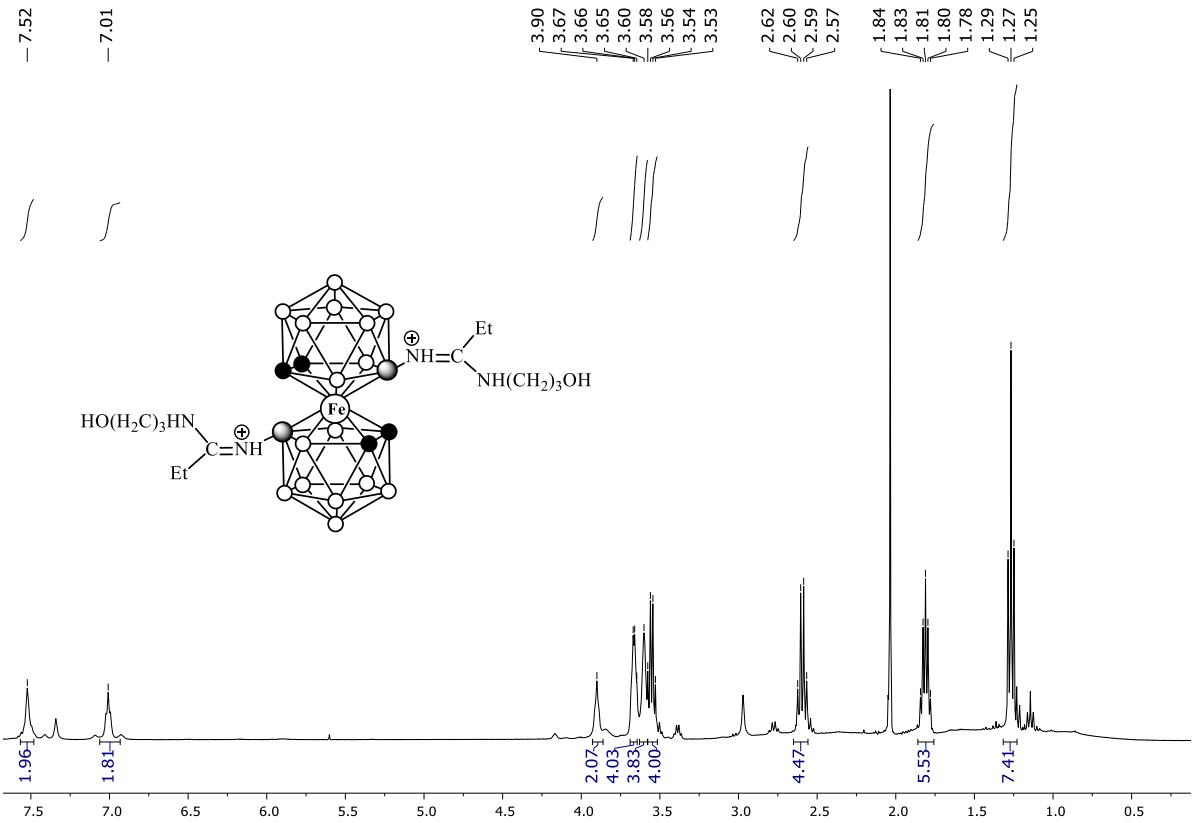

Fig. S17. ^{1}H NMR spectrum of compound **9** (acetone-d_6).

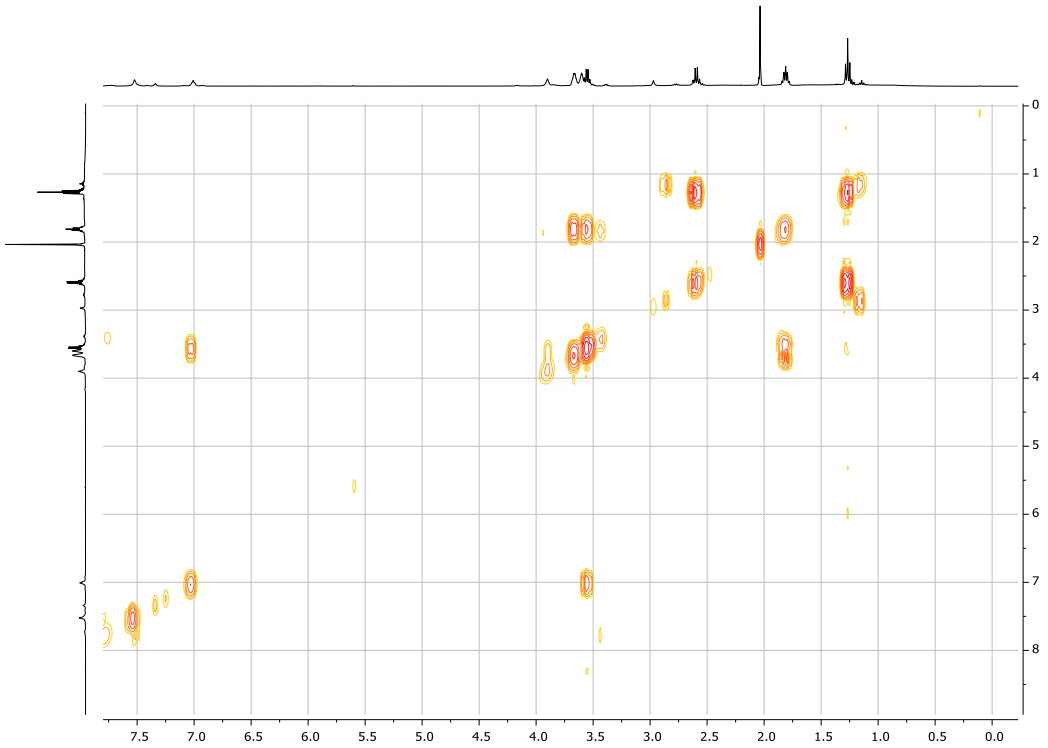

Fig. S18. ^{1}H-^{1}H COSY NMR spectrum of compound **9** (acetone-d_6).

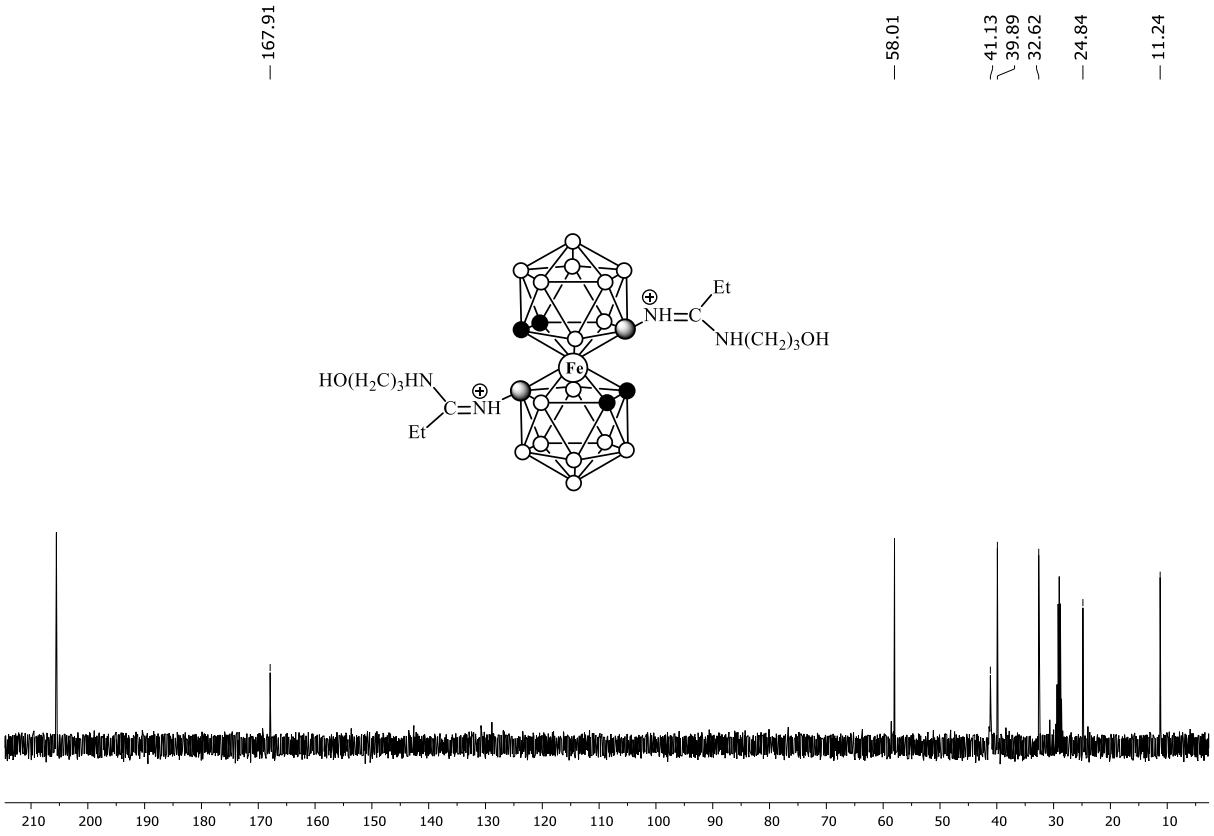

Fig. S19. ^{13}C NMR spectrum of compound **9** (acetone-d_6).

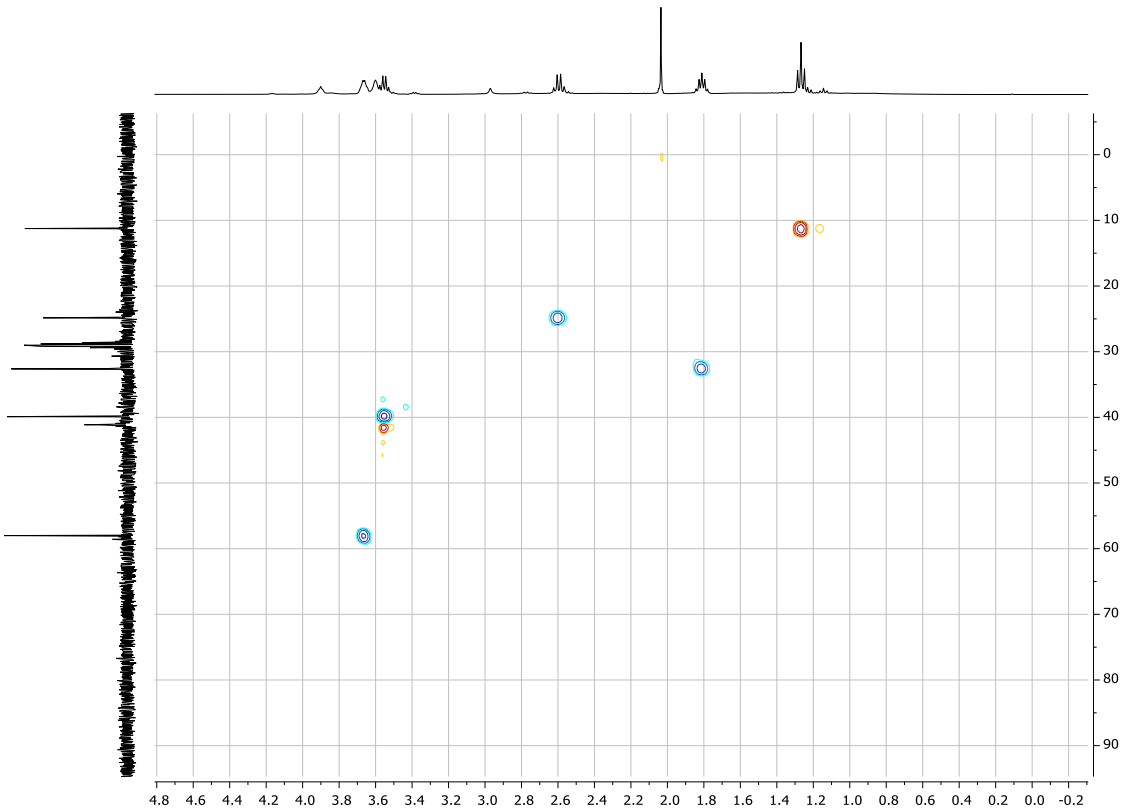

Fig. S20. ^{1}H-^{13}C HSQC NMR spectrum of compound **9** (acetone-d_6).

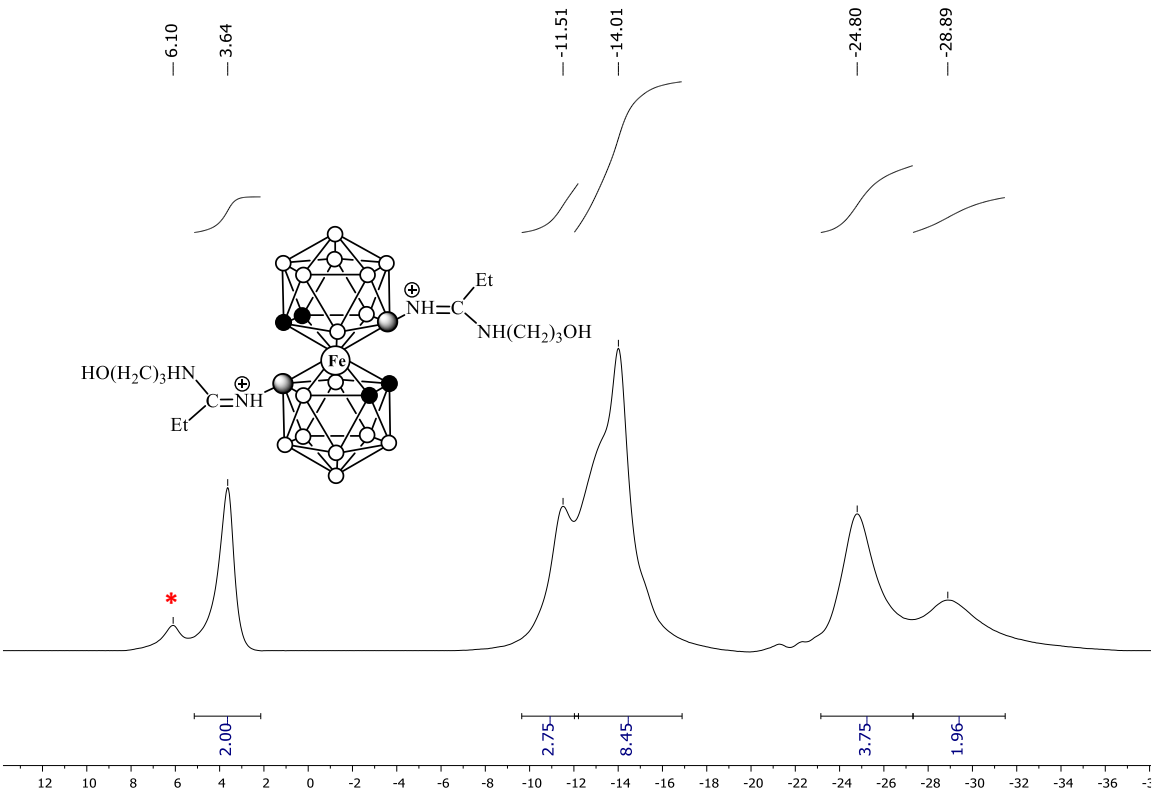

* minor isomers signal

Fig. S21. $^{11}B\{^{1}H\}$ NMR spectrum of compound **9** (acetone-d_6).

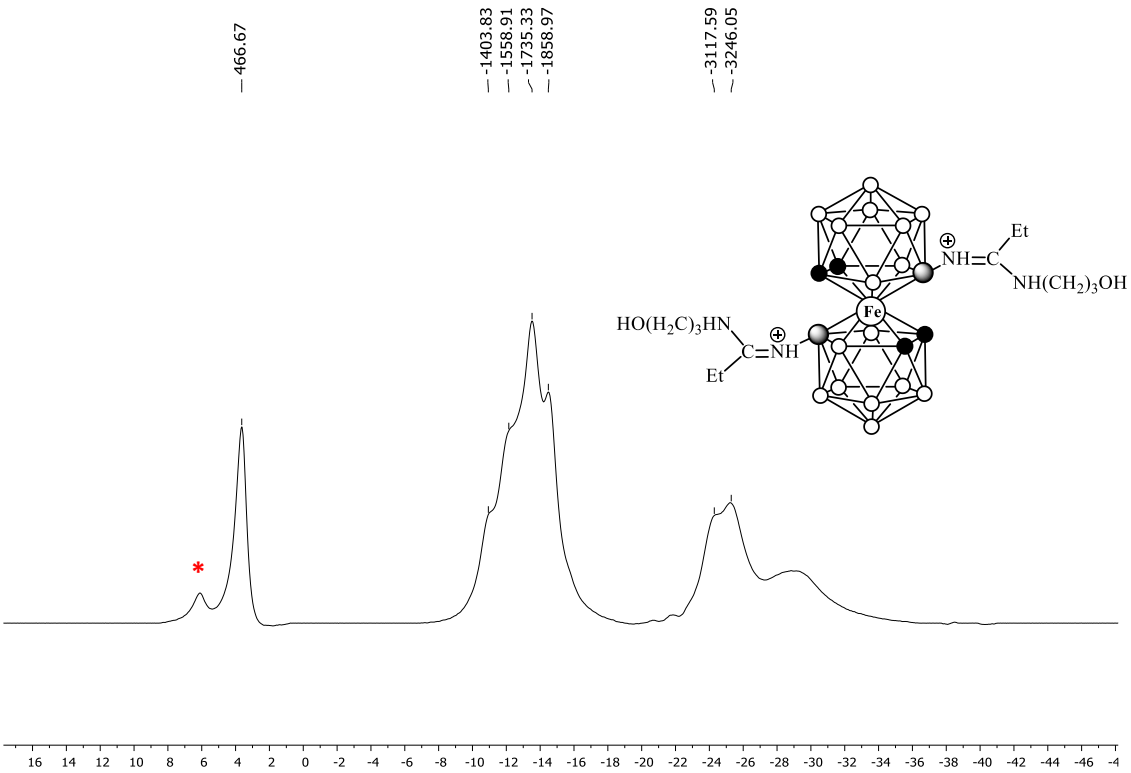

* minor isomers signal

Fig. S22. ^{11}B NMR spectrum of compound **9** (acetone-d_6).

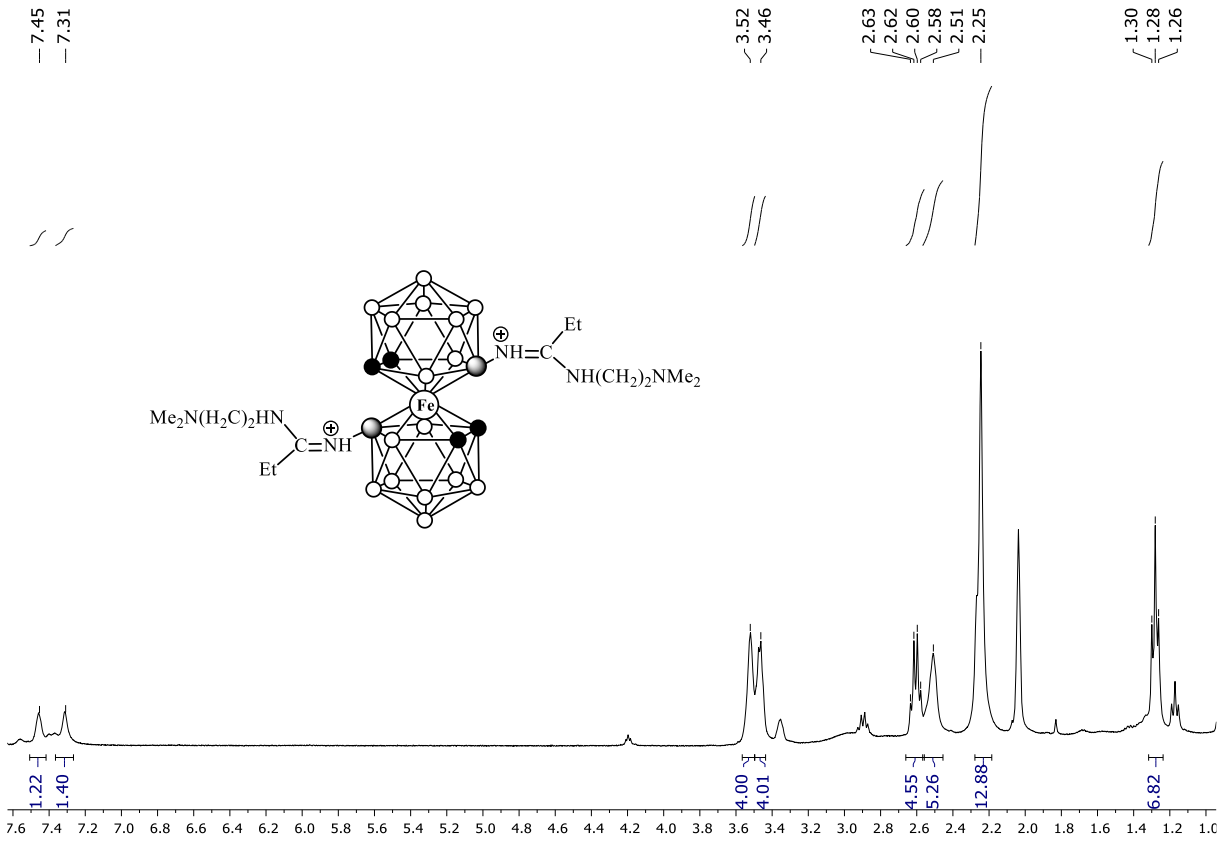

Fig. S23. ^{1}H NMR spectrum of compound **10** (acetone-d_6).

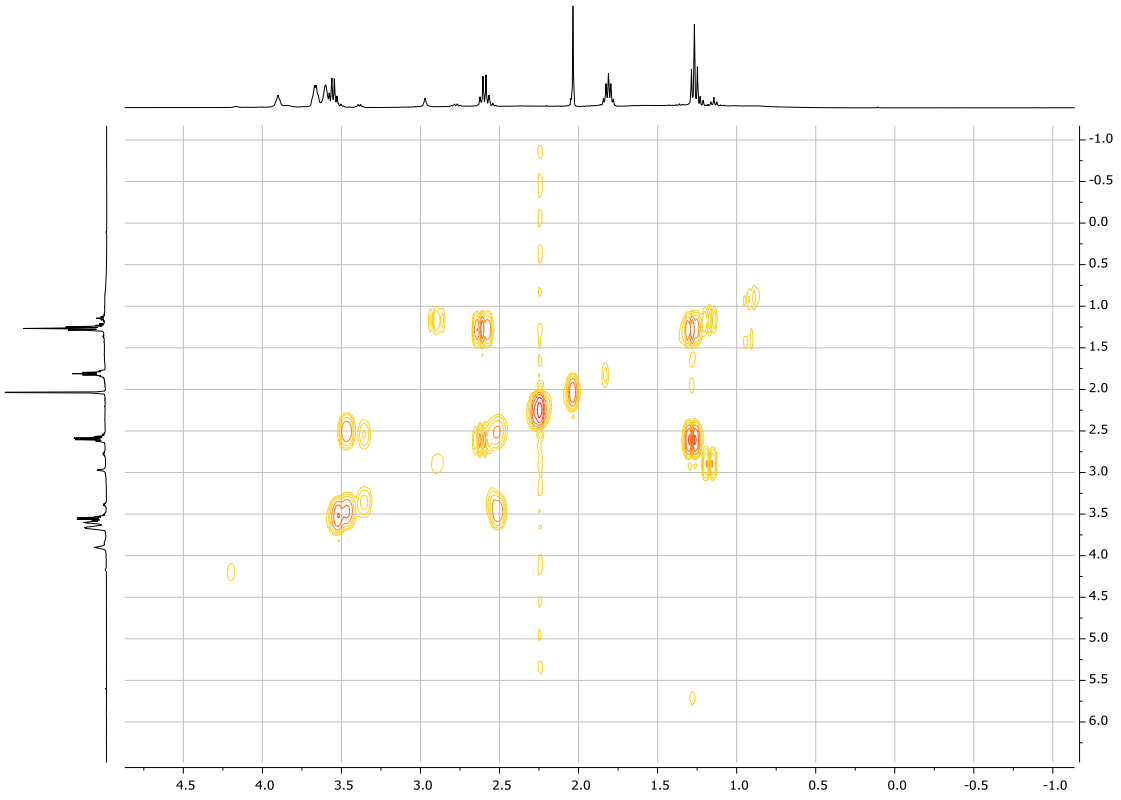

Fig. S24. ^{1}H-^{1}H COSY NMR spectrum of compound **10** (acetone-d_6).

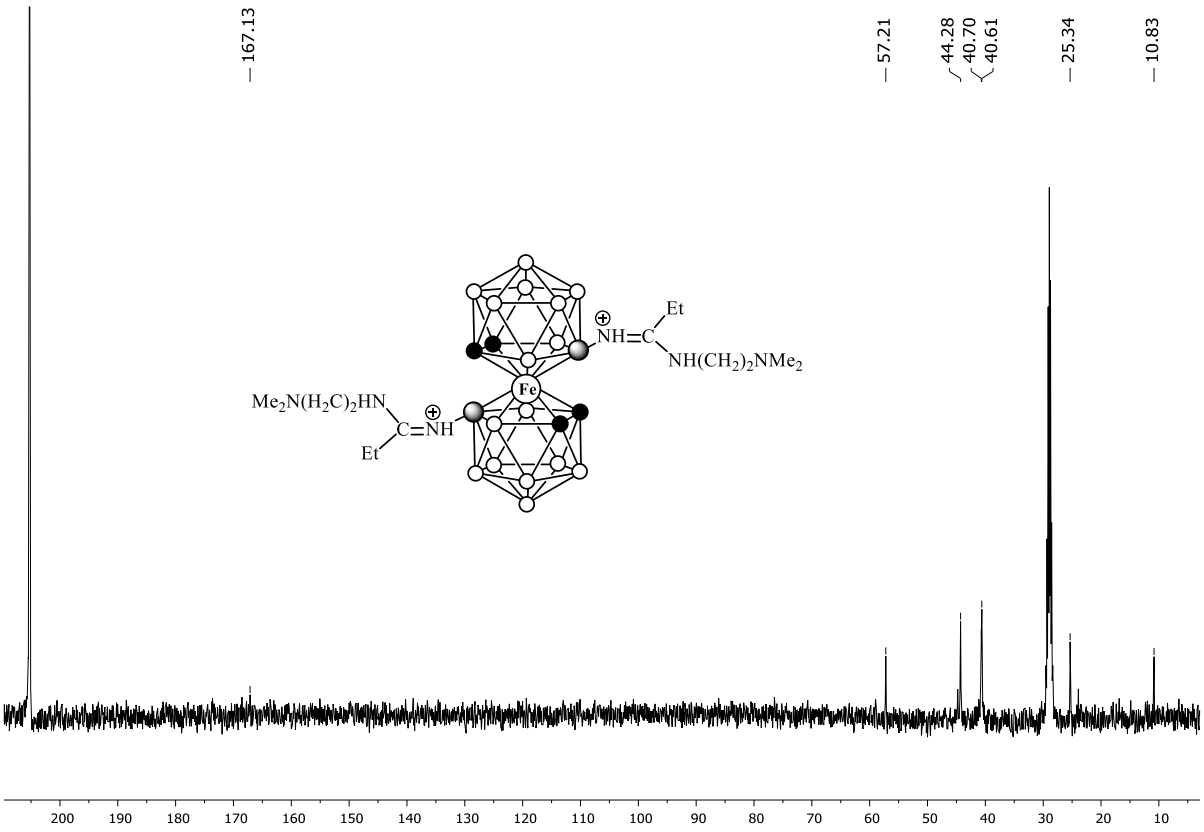

Fig. S25. ^{13}C NMR spectrum of compound **10** (acetone-d_6).

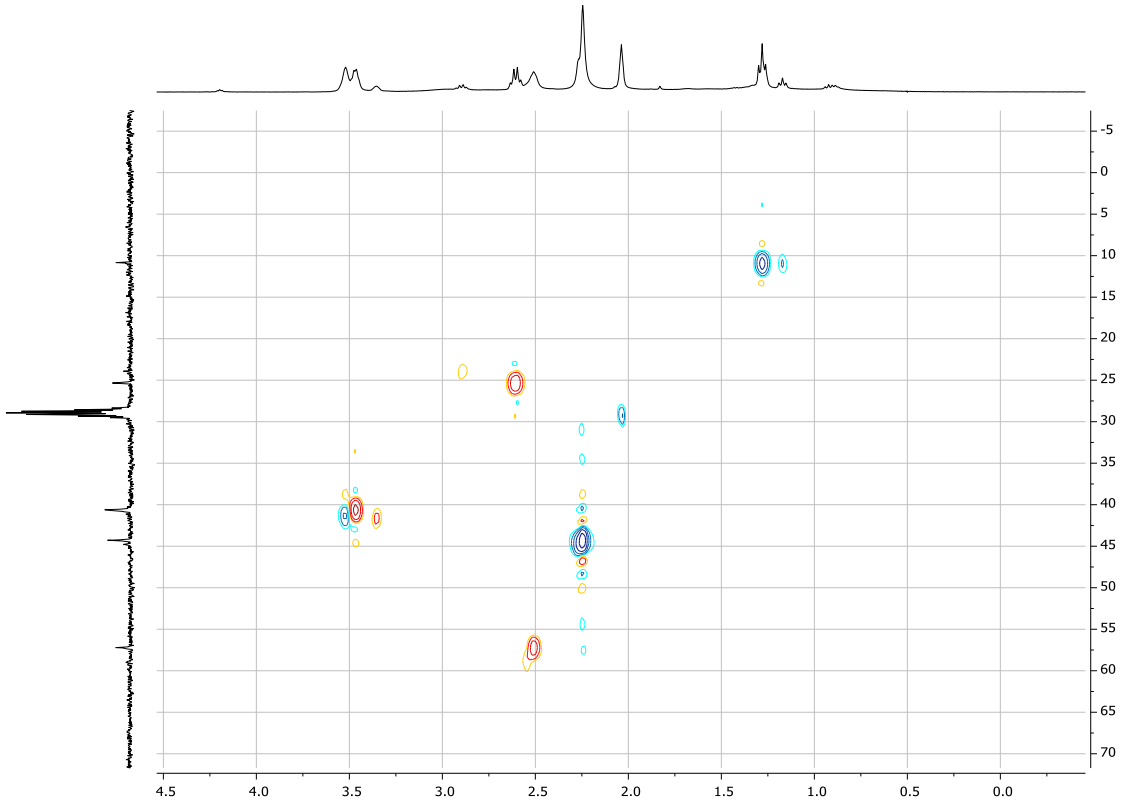

Fig. S26. ^{1}H-^{13}C HSQC NMR spectrum of compound **10** (acetone-d_6).

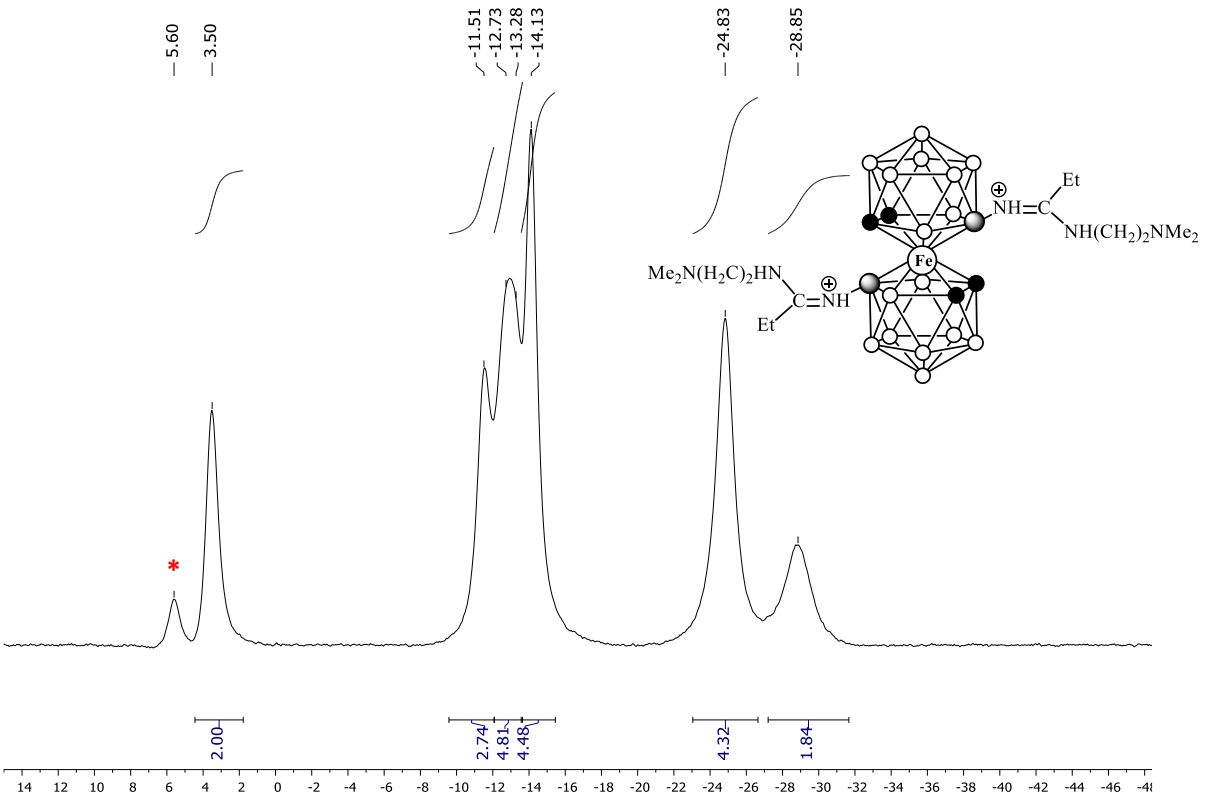

* minor isomers signal

Fig. S27. $^{11}B\{^{1}H\}$ NMR spectrum of compound **10** (acetone-d_6).

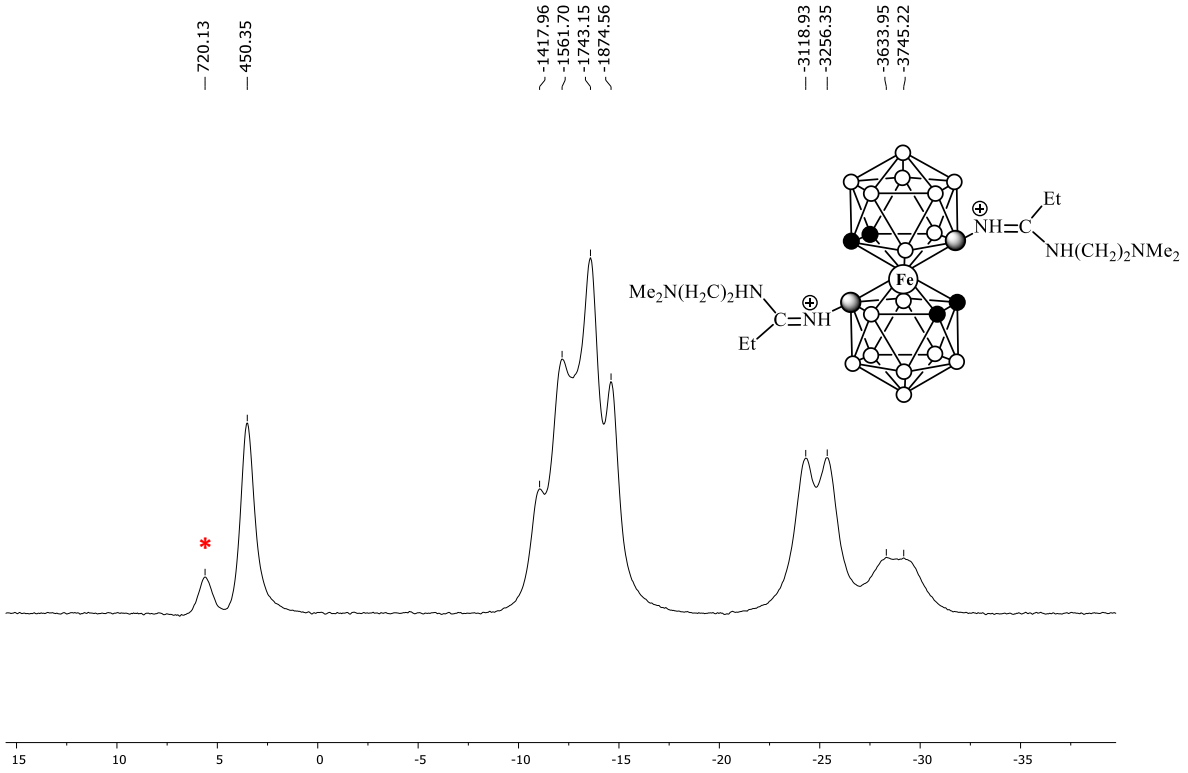

* minor isomers signal

Fig. S28. ^{11}B NMR spectrum of compound **10** (acetone-d_6).

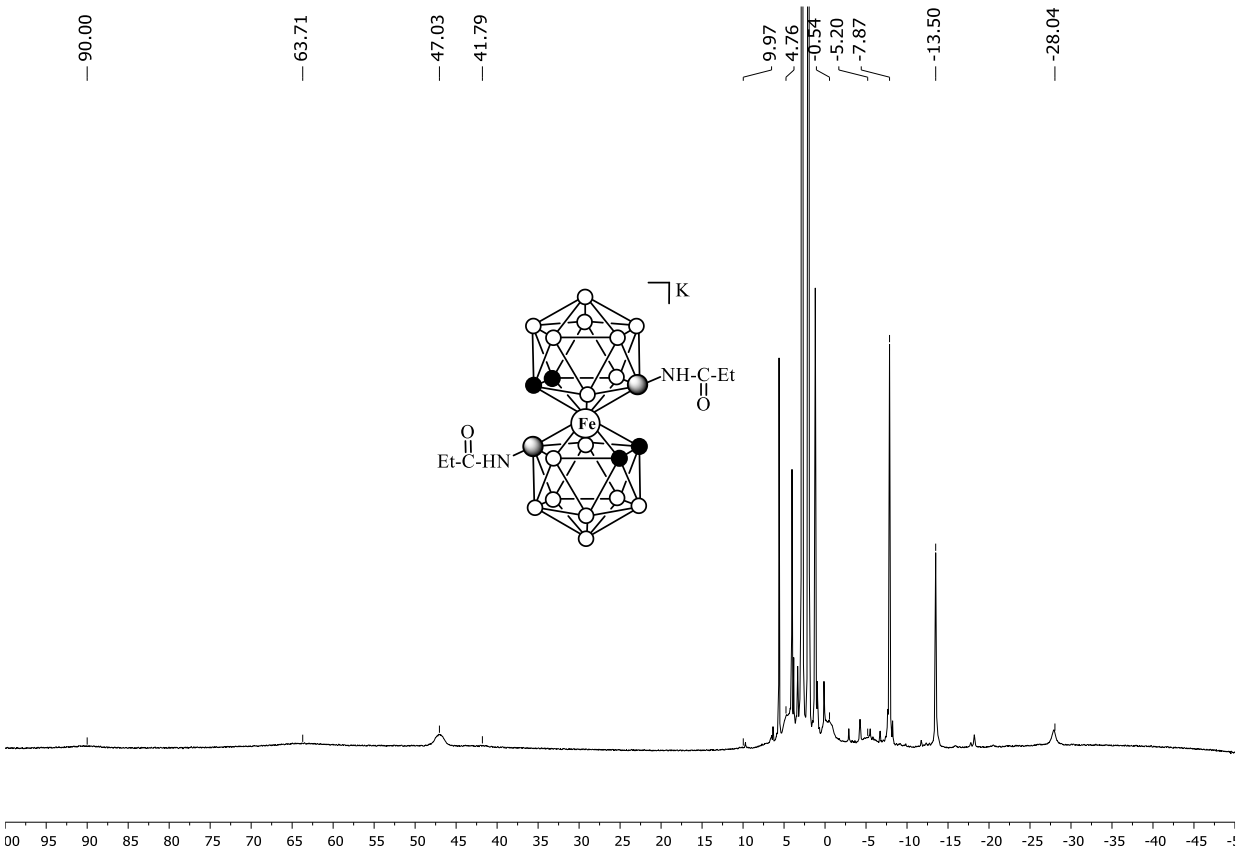

Fig. S29. ^{1}H NMR spectrum of compound **12** (acetone-d_6).

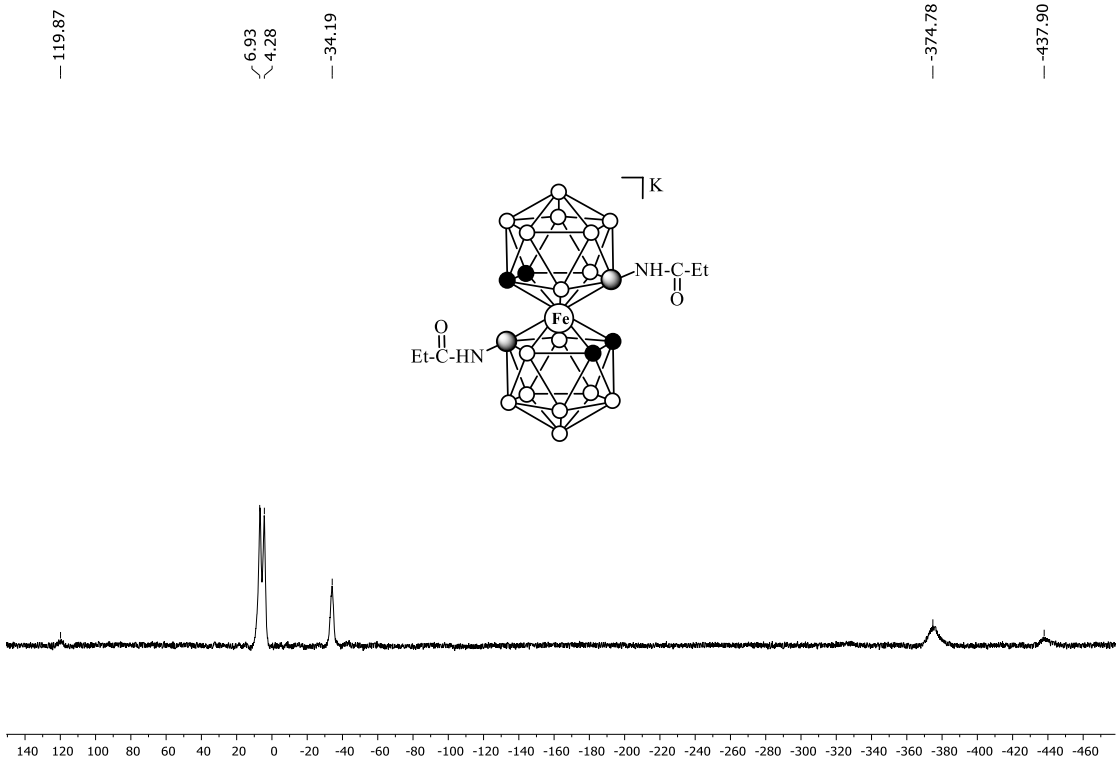

Fig. S30. ^{11}B NMR spectrum of compound **12** (acetone-d_6).

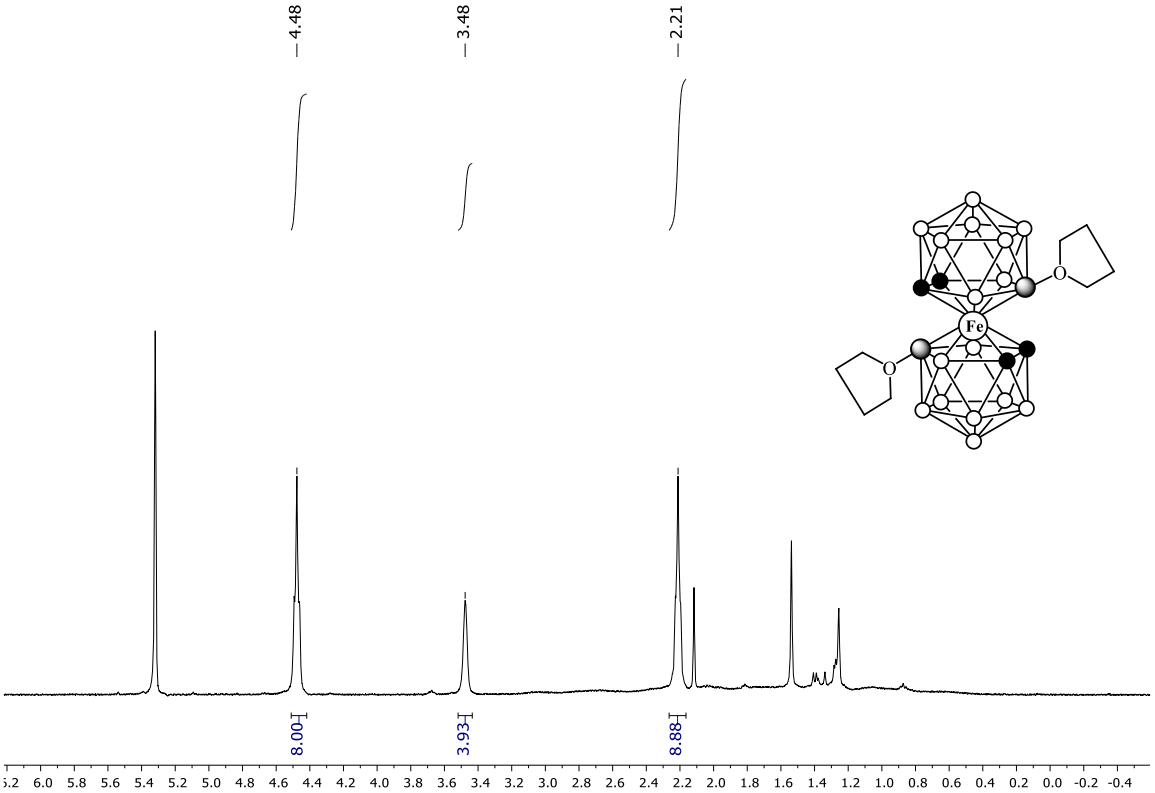

Fig. S31. ^{1}H NMR spectrum of compound **17** (CD_2Cl_2).

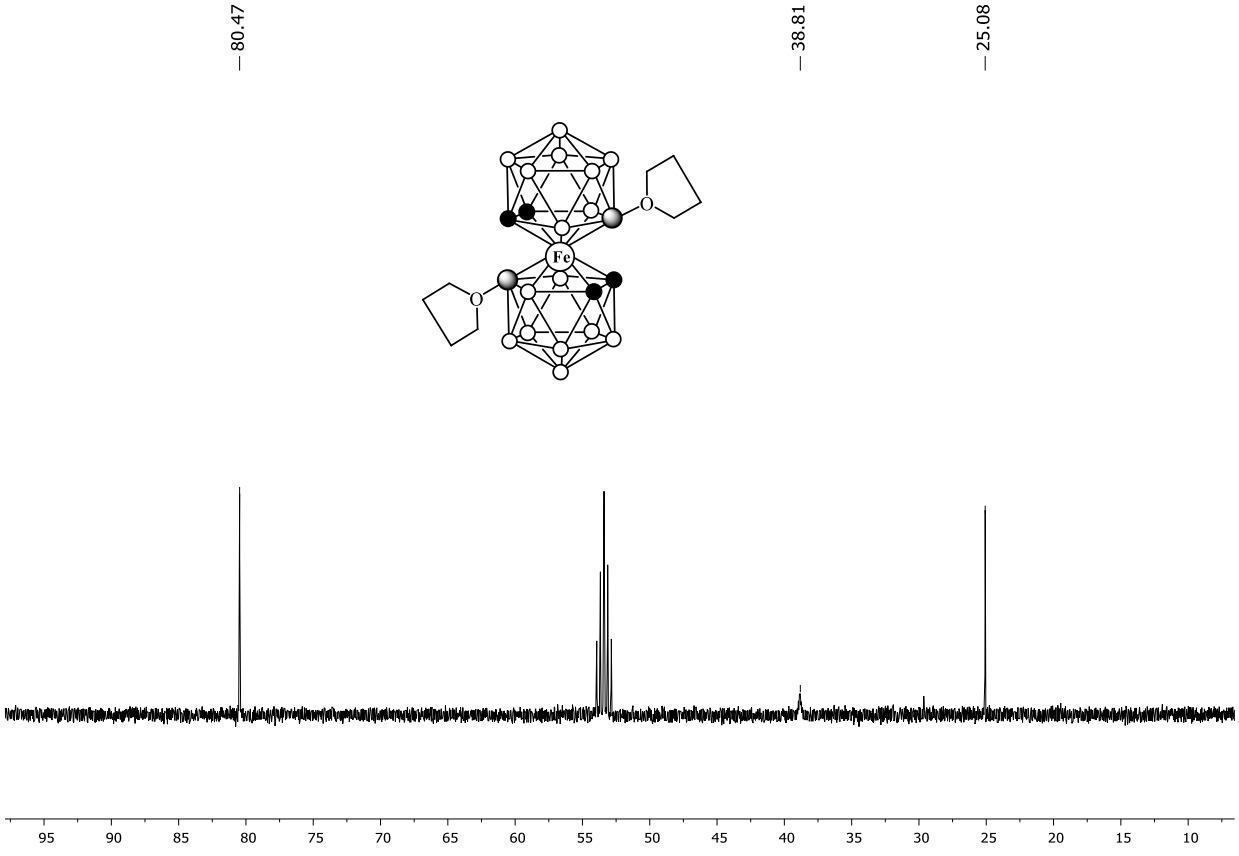

Fig. S32. ^{13}C NMR spectrum of compound **17** (CD_2Cl_2).

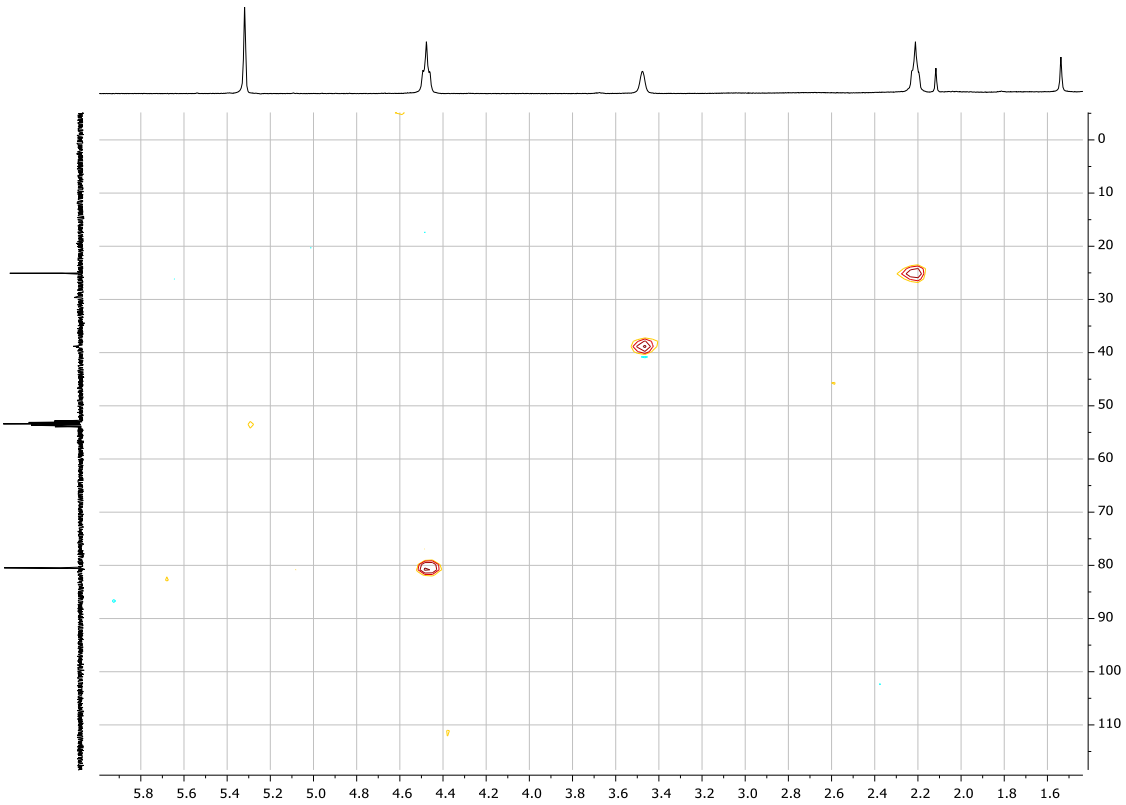

Fig. S33. ^{1}H-^{13}C HSQC NMR spectrum of compound **17** (CD_2Cl_2).

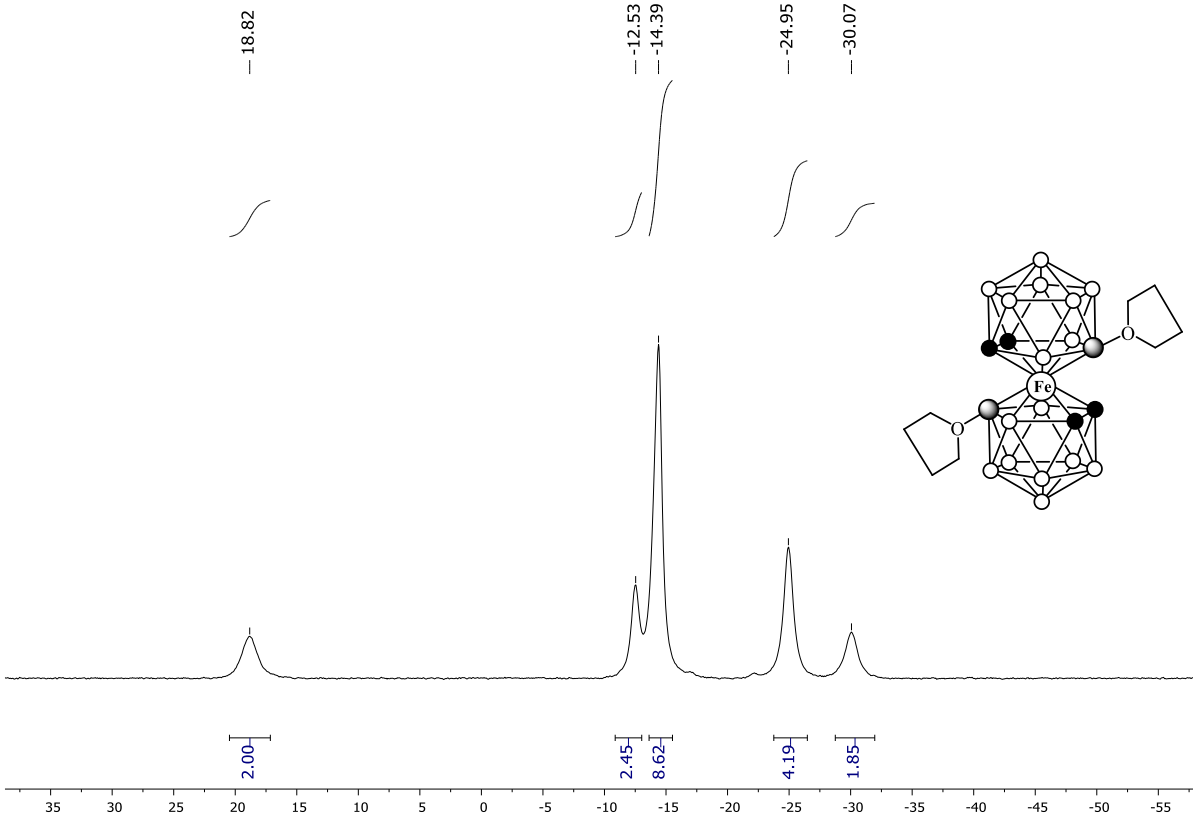

Fig. S34. $^{11}B\{^{1}H\}$ NMR spectrum of compound **17** (CD_2Cl_2).

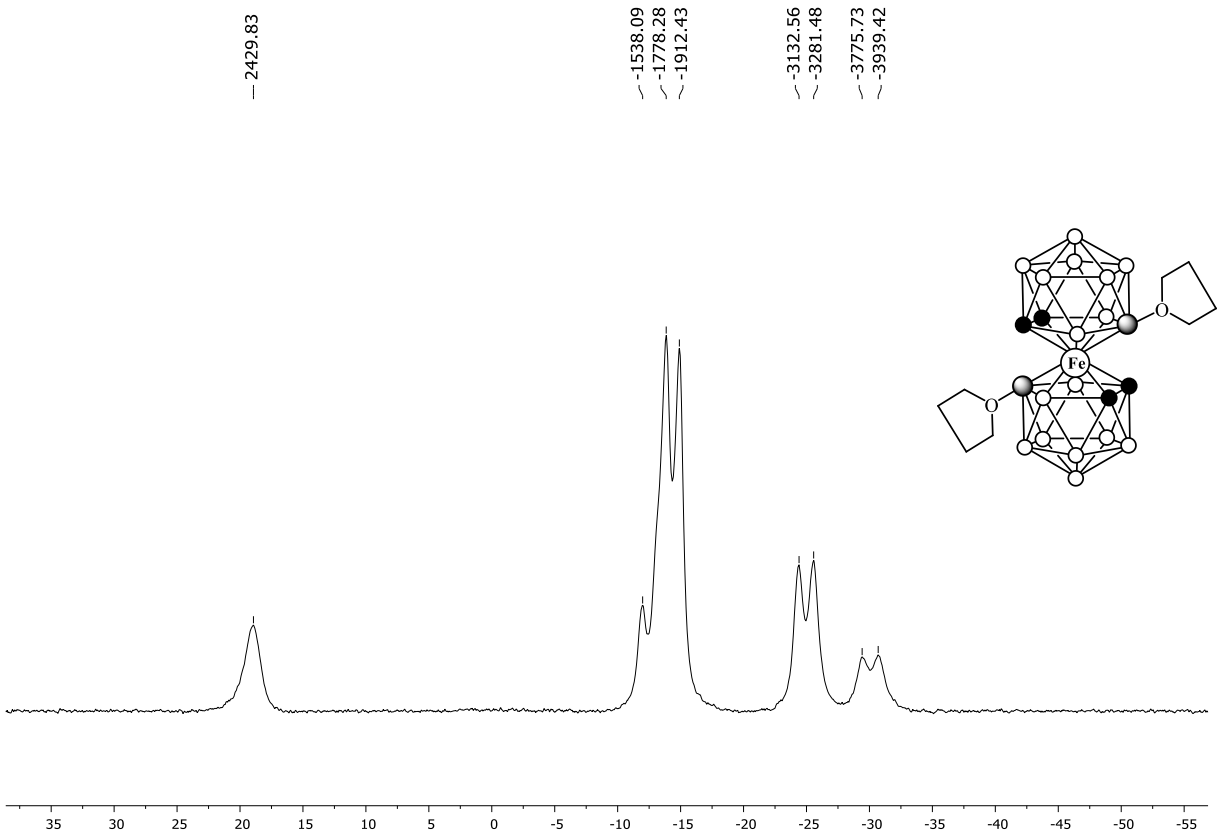

Fig. S35. ^{11}B NMR spectrum of compound **17** (CD_2Cl_2).

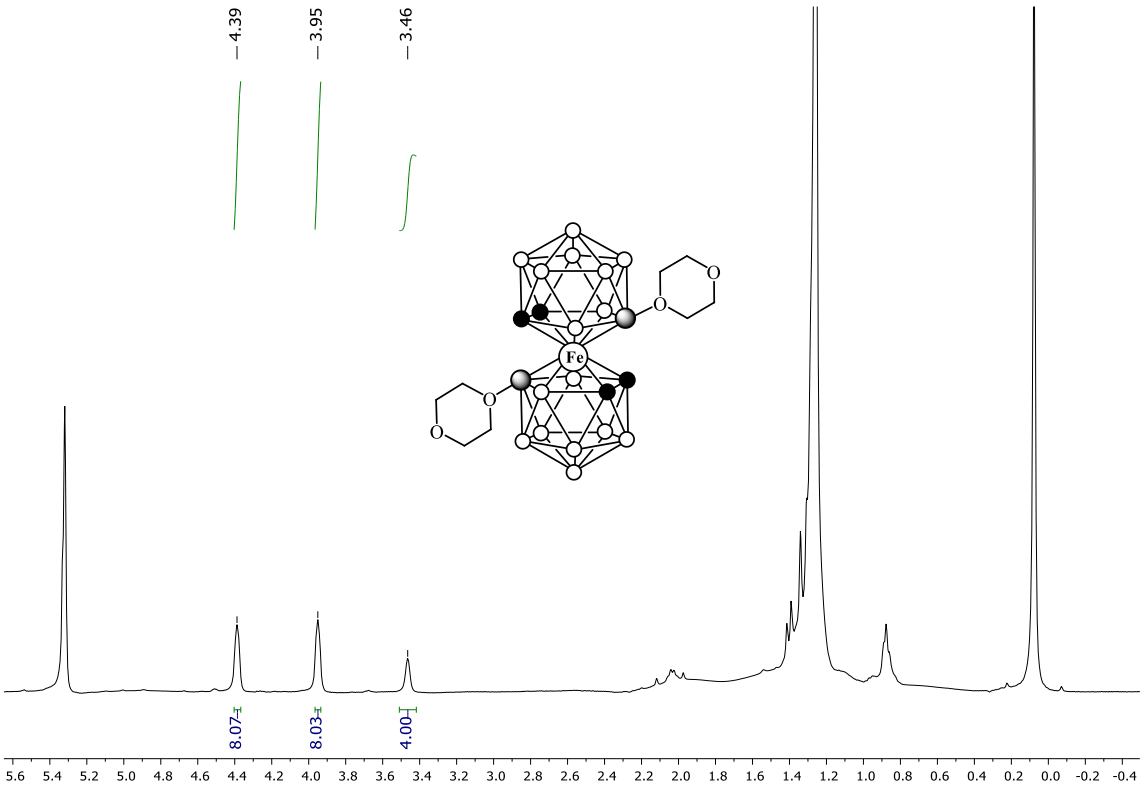

Fig. S31. ^{1}H NMR spectrum of compound **18** (CD_2Cl_2).

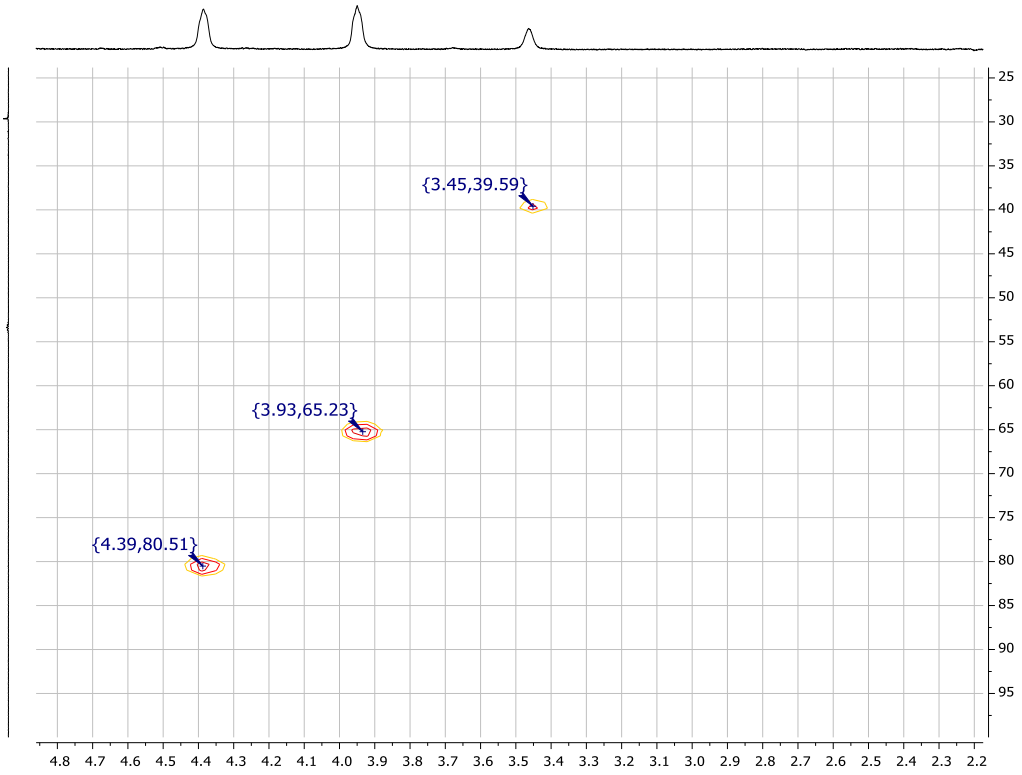

Fig. S32. ^{1}H-^{13}C HSQC NMR spectrum of compound **18** (CD_2Cl_2).

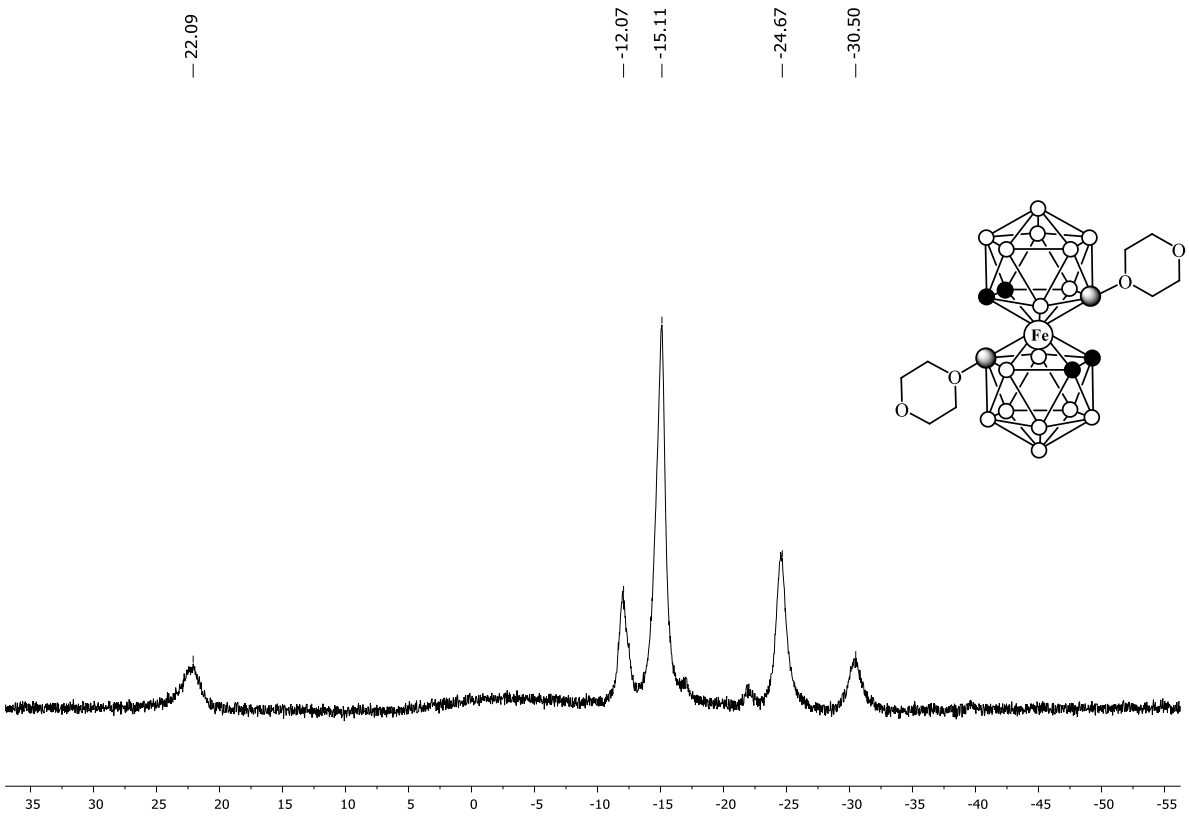

Fig. S33. $^{11}B\{^{1}H\}$ NMR spectrum of compound **18** (CD_2Cl_2).

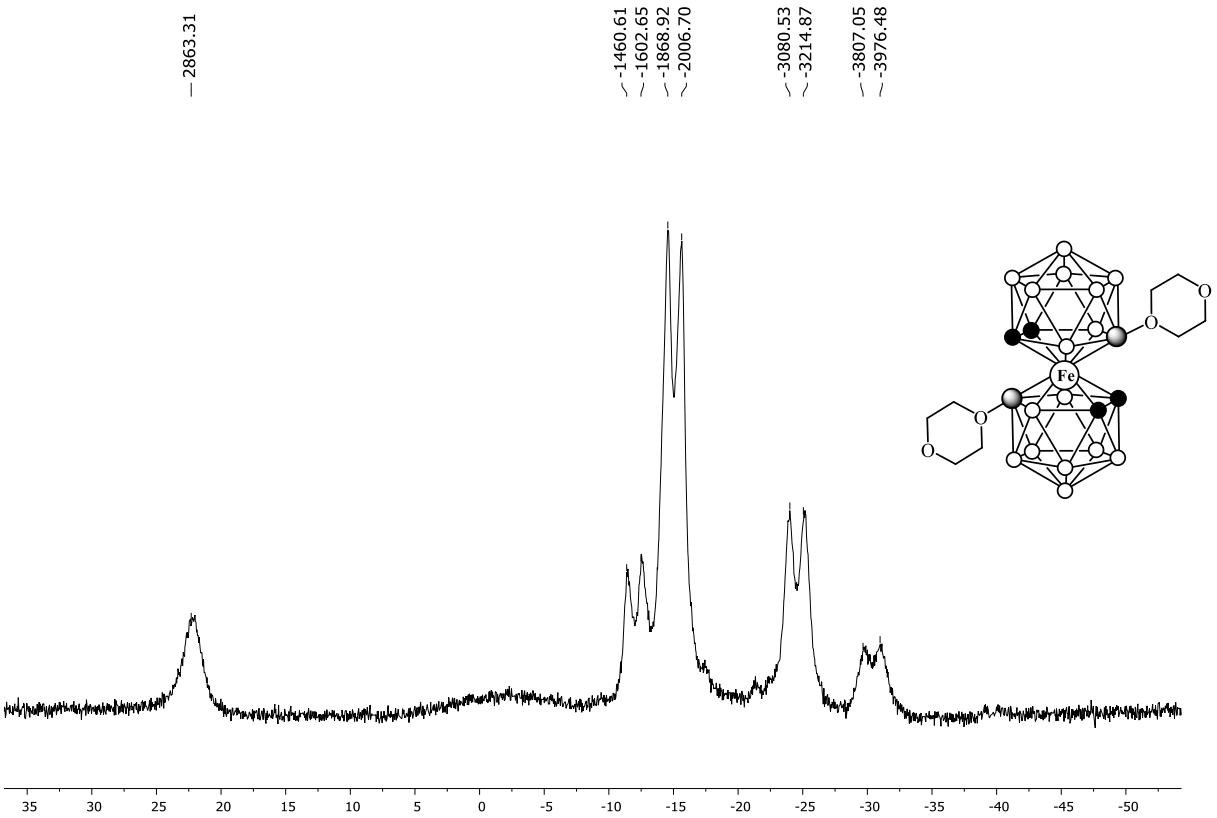

Fig. S34. ^{11}B NMR spectrum of compound **18** (CD_2Cl_2).

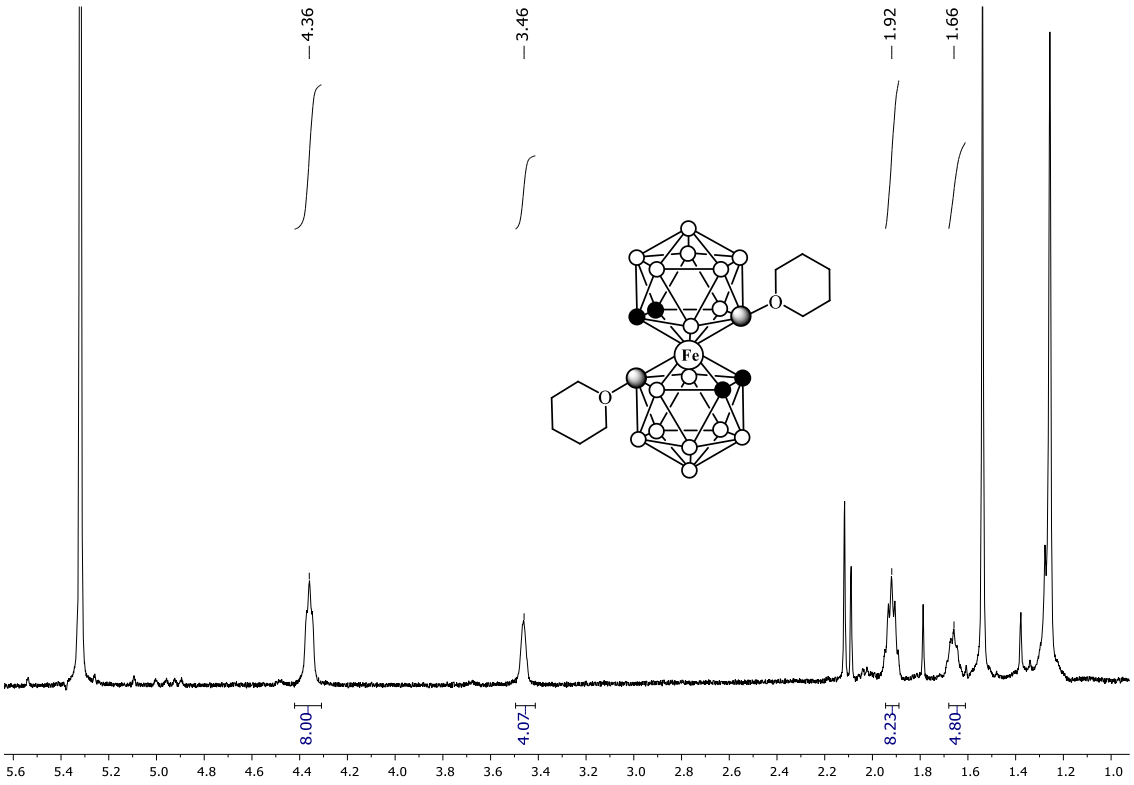

Fig. S35. ^{1}H NMR spectrum of compound **19** (CD_2Cl_2).

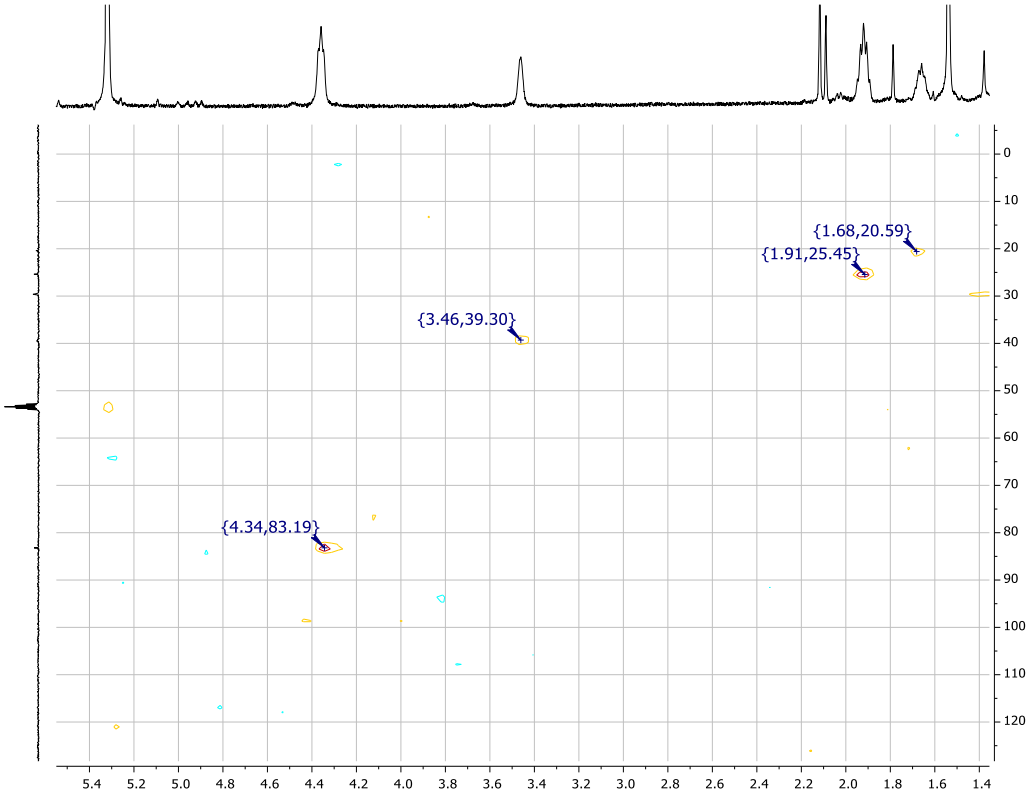

Fig. S36. (HC)HSQC NMR spectrum of compound **19** (CD_2Cl_2).

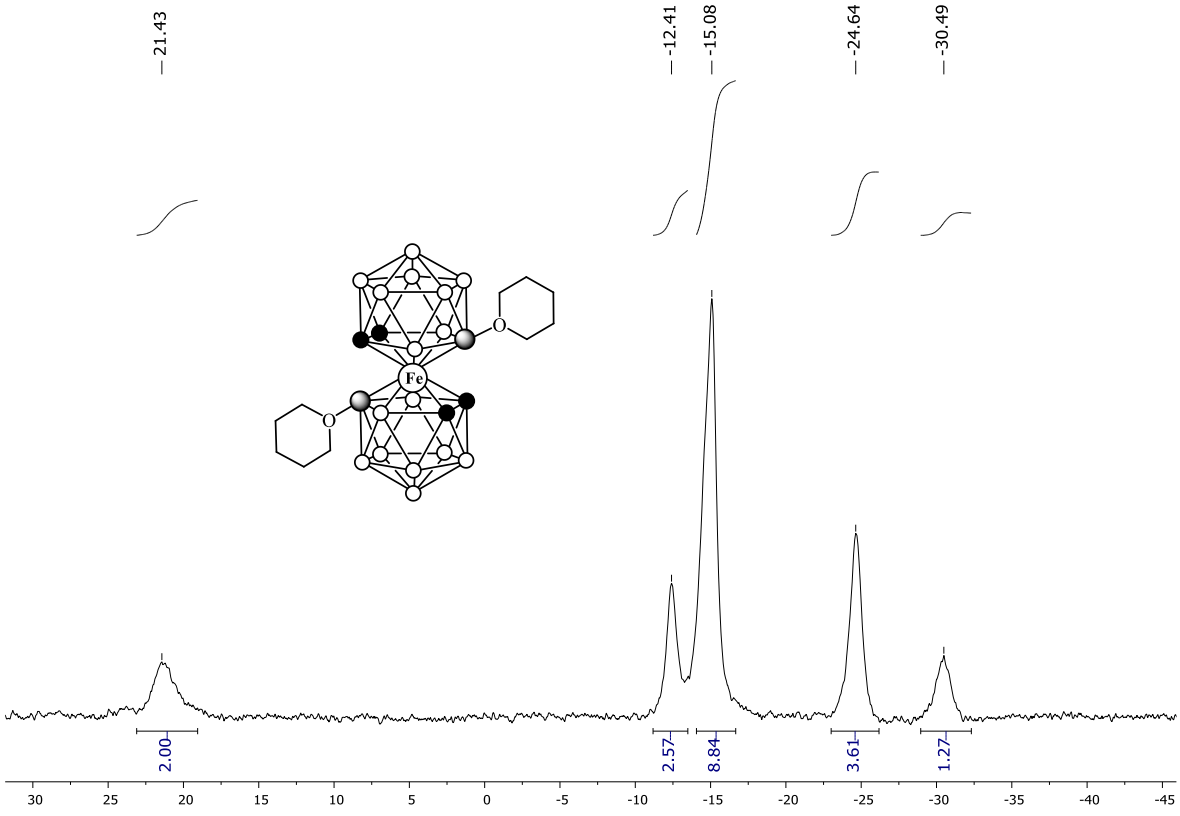

Fig. S37. $^{11}B\{^{1}H\}$ NMR spectrum of compound **19** (CD_2Cl_2).

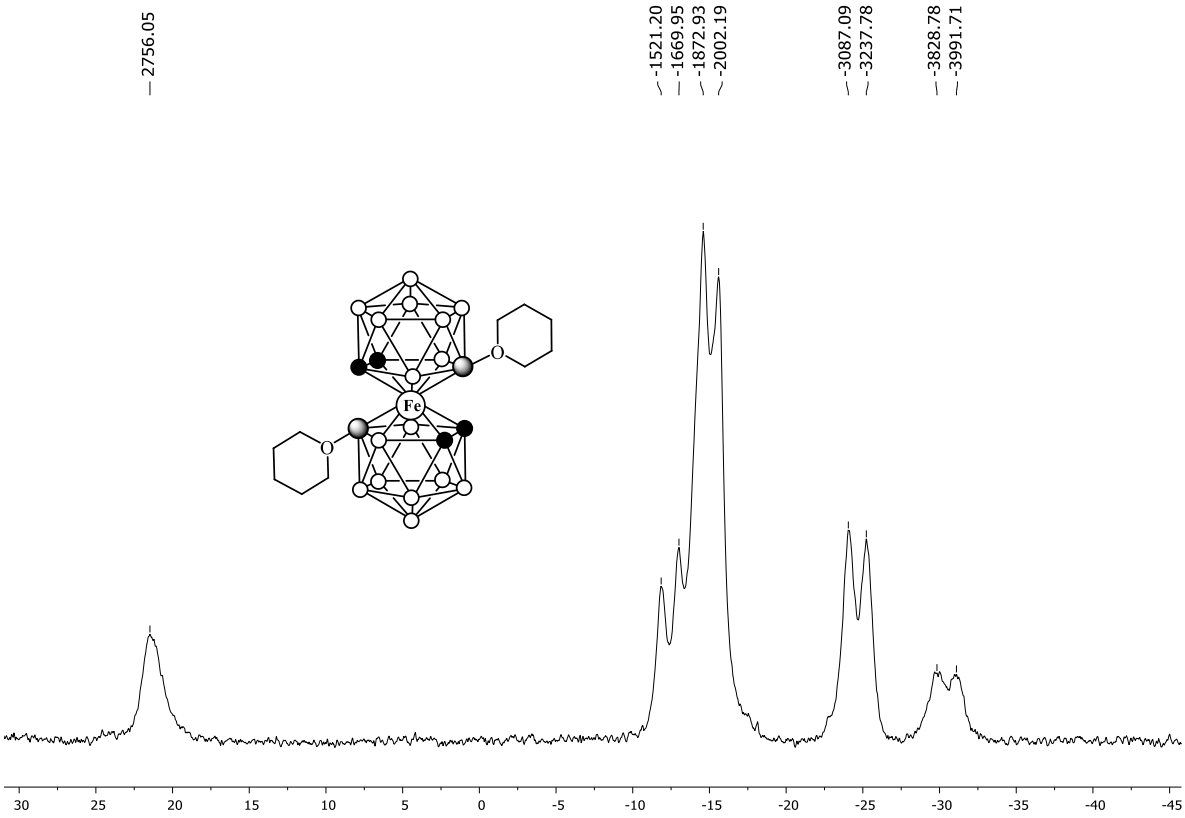

Fig. S38. ^{11}B NMR spectrum of compound **19** (CD_2Cl_2).

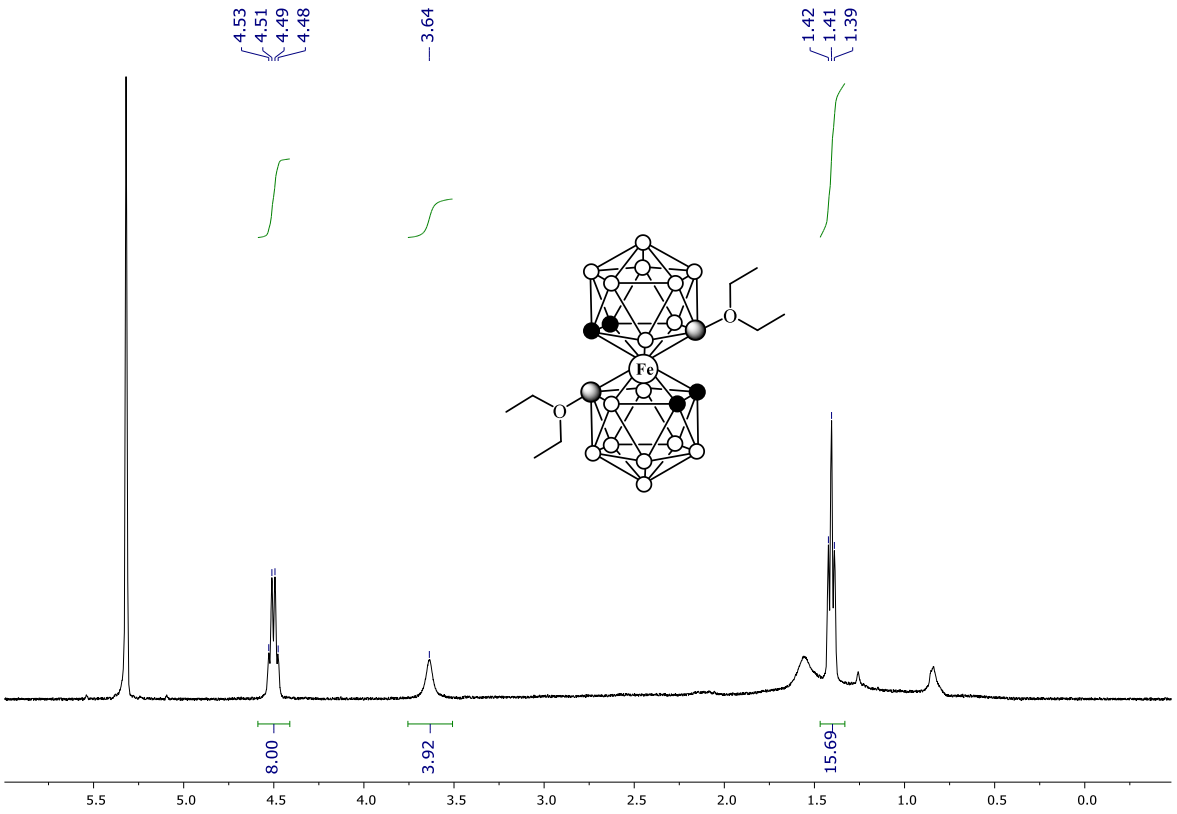

Fig. S39. ^{1}H NMR spectrum of compound **20** (CD_2Cl_2).

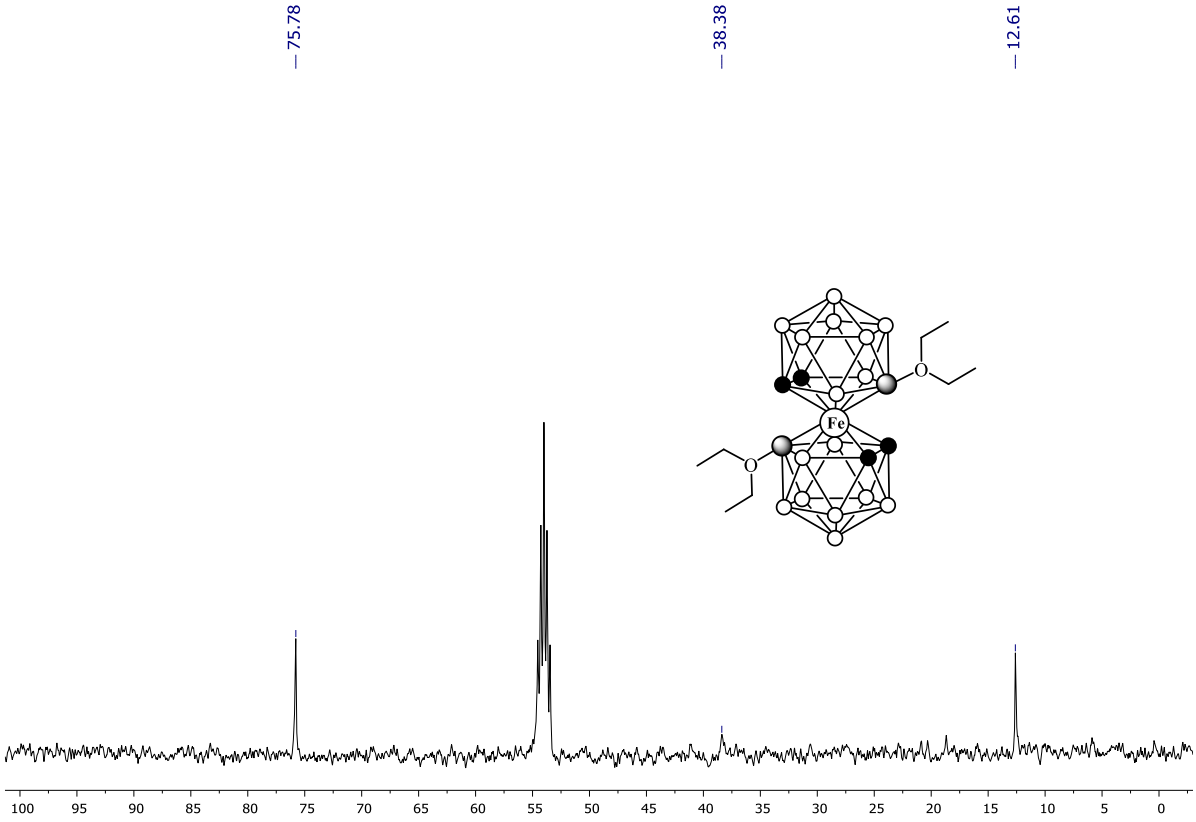

Fig. S40. ^{13}C NMR spectrum of compound **20** (CD_2Cl_2).

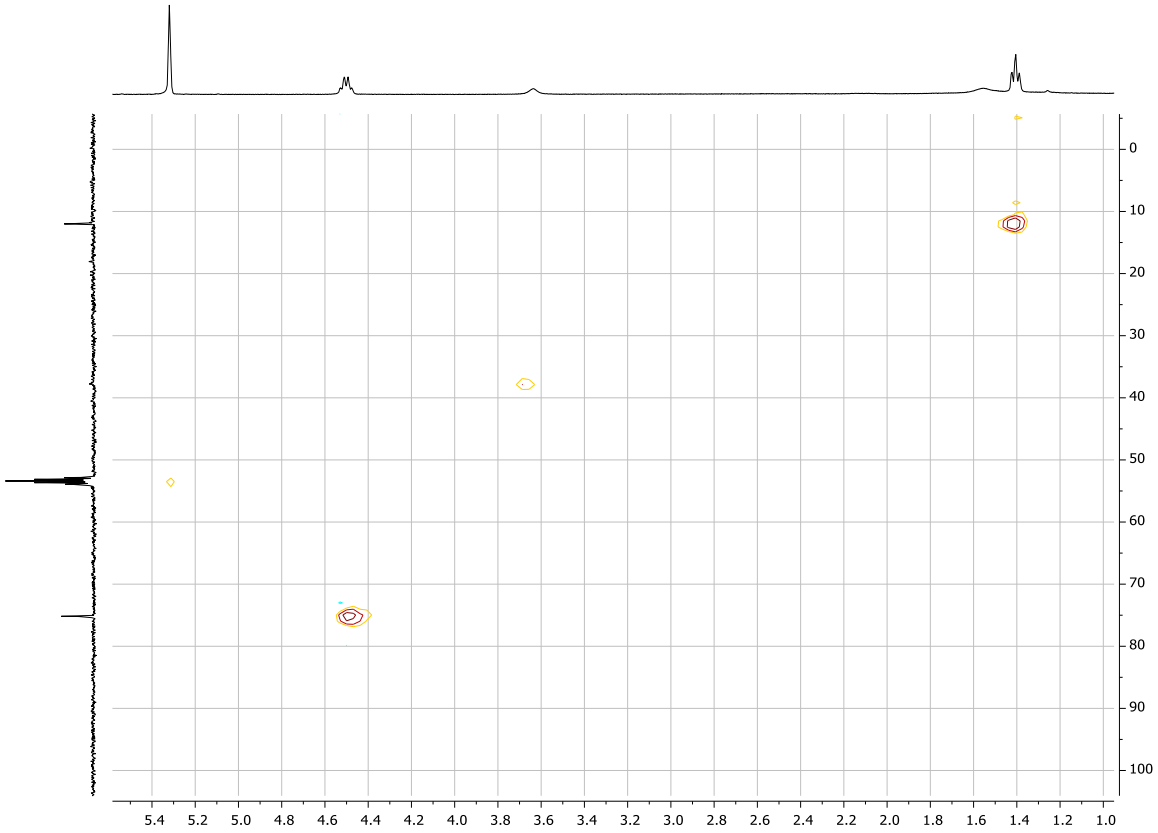

Fig. S41. ^{1}H-^{13}C HSQC NMR spectrum of compound **20** (CD_2Cl_2).

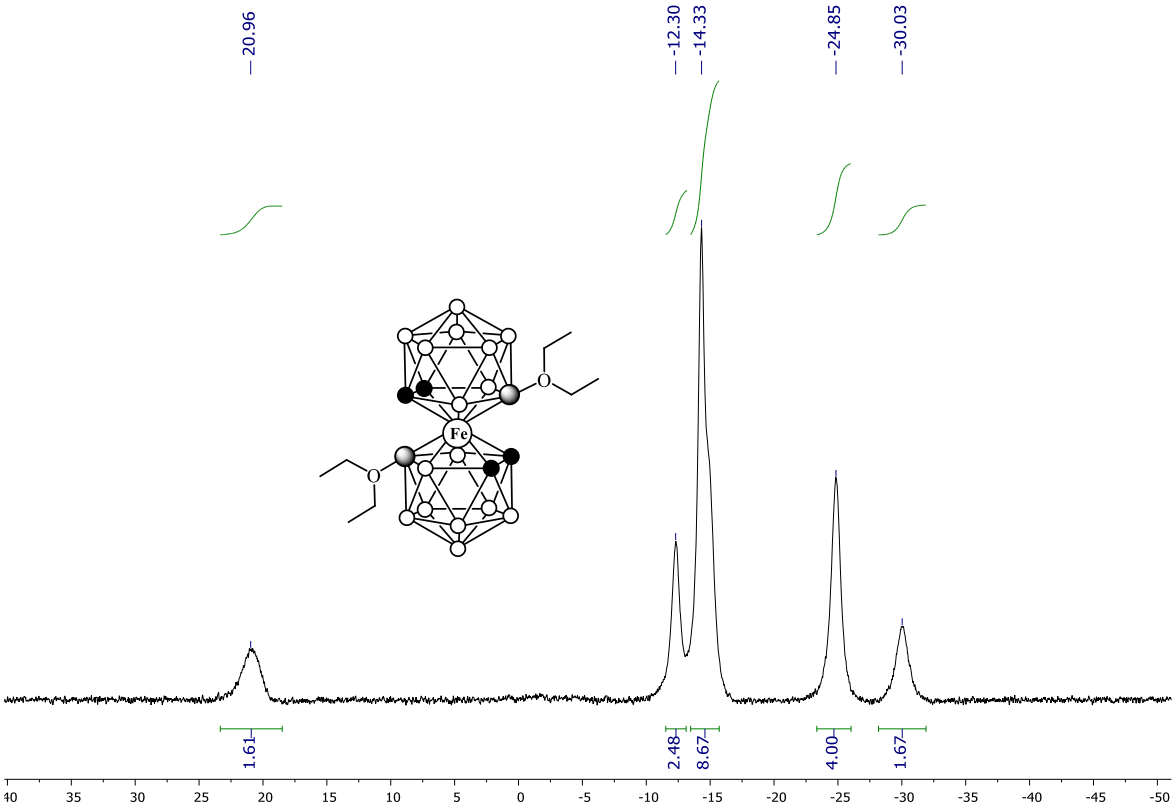

Fig. S42. $^{11}B\{^{1}H\}$ NMR spectrum of compound **20** (CD_2Cl_2).

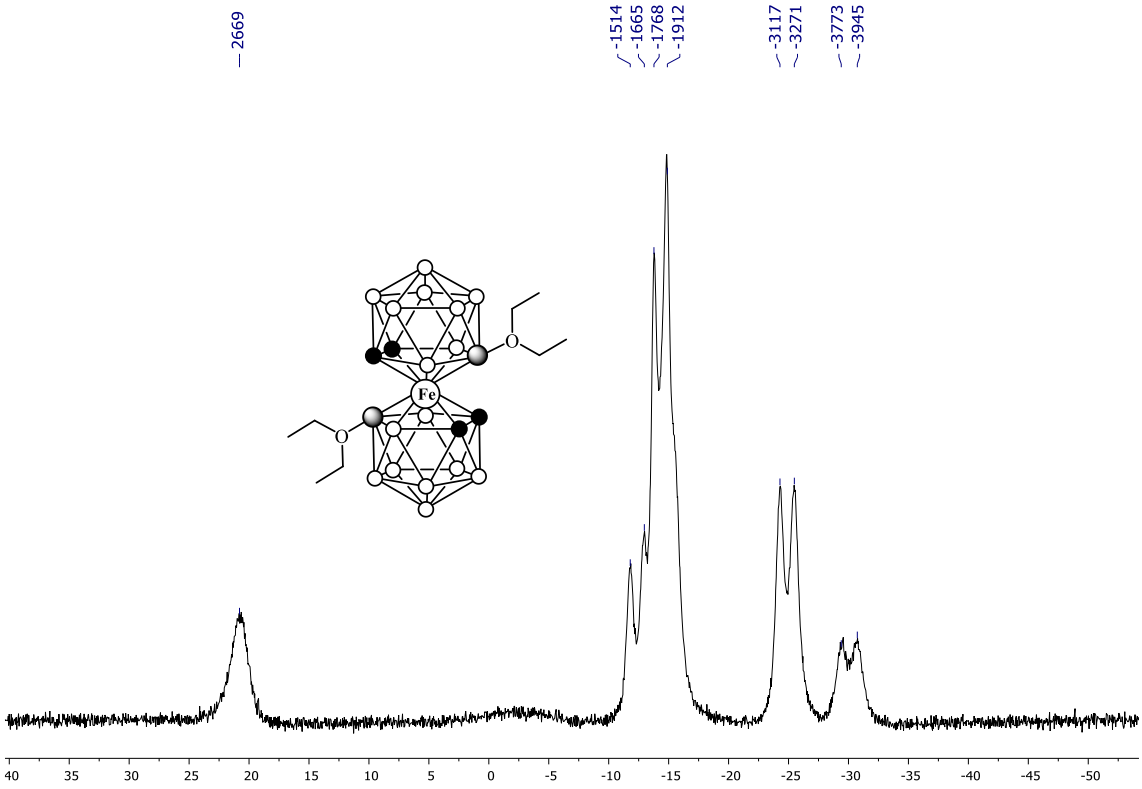

Fig. S43. ^{11}B NMR spectrum of compound **20** (CD_2Cl_2).

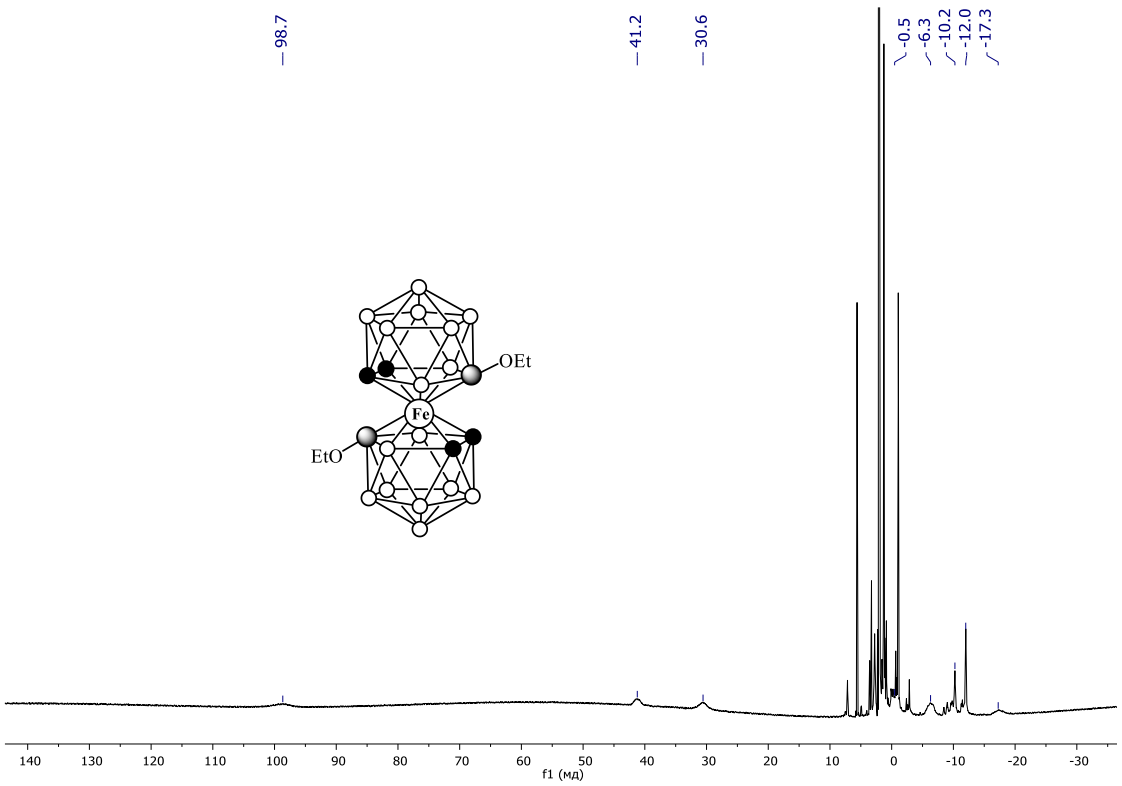

Fig. S44. ^{1}H NMR spectrum of compound **21** (acetone-d_6).

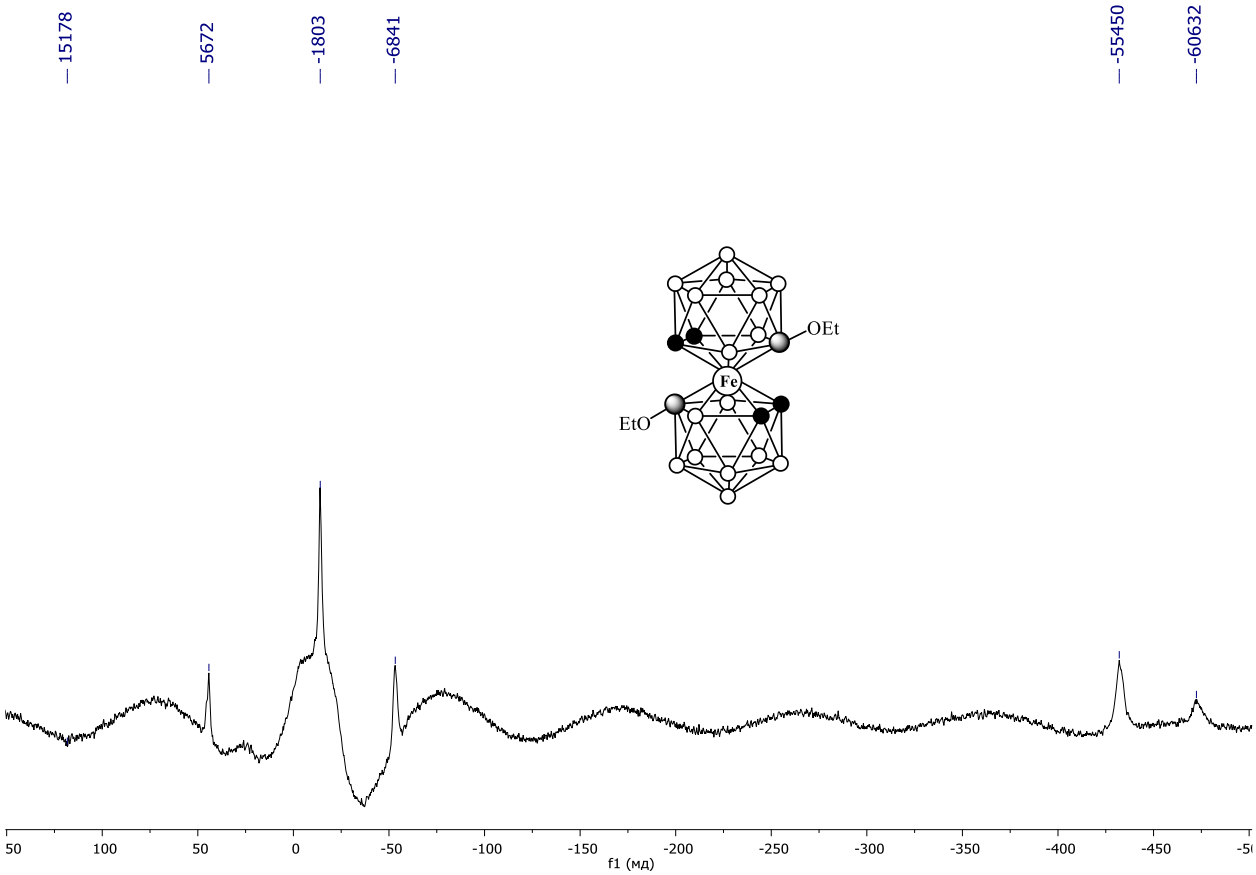

Fig. S45. ^{11}B NMR spectrum of compound **21** (acetone-d_6).

Single Crystal X-Ray Diffraction

Table S1. Crystallographic data for complexes **6** and **9**.

	6	**9**
Formula	$C_{16}H_{48}B_{18}FeN_4$	$C_{16}H_{48}B_{18}FeN_4O_2{\cdot}2(C_3H_6O)$
FW	574.01	695.17
Crystal system	monoclinic	monoclinic
Space group	$P2_1/c$	$P2_1/n$
a, Å	11.7267(3)	9.237(3)
b, Å	9.3910(3)	14.462(5)
c, Å	13.8172(4)	13.944(4)
β, deg.	109.0480(10)	95.624(10)
V, Å^3	1438.31(7)	1853.6(11)
Z	2	2
ρ_{calc}, g·cm^{-3}	1.263	1.246
F(000)	576	736
μ, mm^{-1}	0.542	0.443
θ range, deg.	2.67–27.16	2.82 – 27.23
Reflections collected	20067	26327
Independent reflns. / R_{int}	3175/0.1055	4106/0.0503
Completeness to theta θ, %	99.7	99.1
Ref. parameters	228	278
GOF (F^2)	1.059	1.130
Reflections with $I>2\sigma(I)$	2436	3363
$R_1(F)$ ($I>2\sigma(I)$)[a]	0.0327	0.0310
$wR_2(F^2)$ (all data)[b]	0.0820	0.0827
Largest diff. peak/hole, *e*·Å^{-3}	0.385/-0.313	0.326/-0.255
CCDC Number	2278478	2278479

[a] $R_1 = \sum|F_o - |F_c||/\sum(F_o)$; [b] $wR_2 = (\sum[w(F_o^2 - F_c^2)^2]/\sum[w(F_o^2)^2]^{½}$

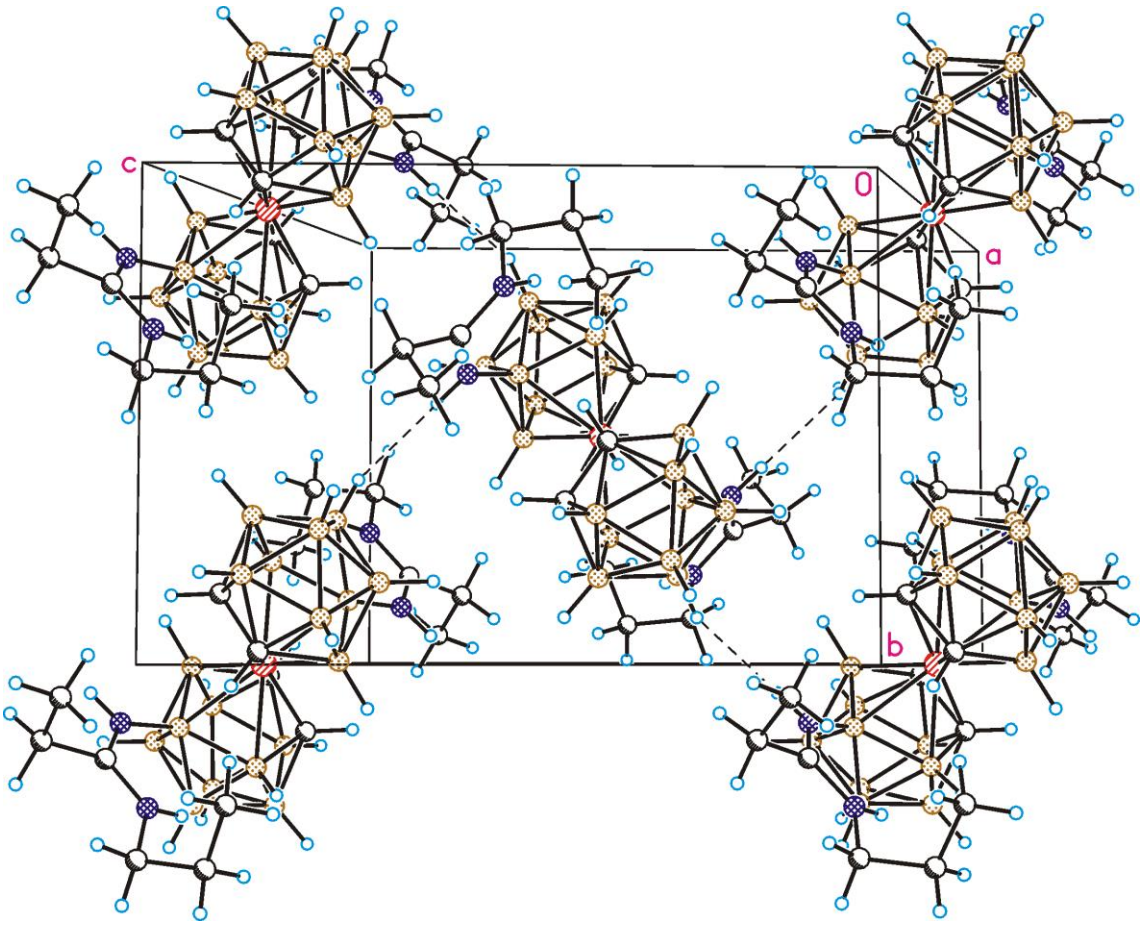

Fig. S46. Fragment of crystal packing in complex [8,8’-(PrNHC(Et)=HN)$_2$-3,3’-Fe(1,2-$C_2B_9H_{10}$)$_2$] (**6**).

Table S2. Crystallographic data for complexes **17**-**20**.

	19	**18**	**17**	**20**
Formula	$C_{14}H_{40}B_{18}FeO_2$	$C_{12}H_{36}B_{18}FeO_4$	$C_{12}H_{36}B_{18}FeO_2$	$C_{12}H_{40}B_{18}FeO_2$
FW	490.89	494.84	462.84	466.87
Crystal system	triclinic	monoclinic	monoclinic	monoclinic
Space group	*P*-1	$P2_1/c$	$P2_1/c$	*Cc*
a, Å	7.1922(4)	10.3079(6)	20.0972(18)	13.5862(8)
b, Å	9.3870(5)	7.8554(5)	8.3625(8)	19.2934(11)
c, Å	9.7241(5)	14.9390(9)	13.9406(12)	9.7040(5)
α, deg.	83.2196(16)	90	90	90
β, deg.	79.4482(16)	98.053(2)	90.145(4)	93.0356(18)
γ, deg.	79.3657(16)	90	90	90
V, Å^3	631.90(6)	1197.72(13)	2342.9(4)	2540.1(2)
Z	1	2	4	4
ρ_{calc}, g·cm^{-3}	1.290	1.372	1.312	1.221
F(000)	256	512	960	976
μ, mm^{-1}	0.611	0.0682	0.655	0.604
θ range, deg.	2.22 – 27.20	3.44 – 26.04	1.46 – 26.87	2.73 – 27.02
Reflns. collected	9381	11730	25314	2773
Indep. reflns. / R_{int}	2801/0.0406	2353/0.0682	5039/0.0952	2773/0.0807
Completeness to theta θ, %	99.3	99.6	99.7	99.7
Ref. parameters	200	200	299	302
GOF (F^2)	1.077	1.035	0.993	0.987
Rflns with $I>2\sigma(I)$	2407	1711	3844	2111
$R_1(F)$ ($I>2\sigma(I)$)[a]	0.0335	0.0344	0.0589	0.0397
$wR_2(F^2)$ (all data)[b]	0.0813	0.0857	0.1555	0.0899
Largest diff. peak/hole, *e*·Å^{-3}	0.305/-0.294	0.361/-0.390	0.832/-1.064	0.336/-0.524
CCDC Number	2278480	2278481	2278482	2278483

[a] $R_1 = \sum|F_o - |F_c||/\sum(F_o)$; [b] $wR_2 = (\sum[w(F_o^2 - F_c^2)^2]/\sum[w(F_o^2)^2]^{½}$

Quantum Chemical Calculations

In order to study an influence of the crystal packing on molecular conformation, we calculated molecular geometries of complexes **6** and **9** followed by topological analysis of their electron densities. From Table S2, it is seen that geometries of substituents and their relative orientation is nearly the same for both calculated molecules as well as for X-ray structure of complex **6**. The only exception is the difference in C3-N2-C6-C7 torsion angle (~ 25°) that is related to a formation of quite weak H4···H8B and H7C···H8B contacts in the isolated molecule of complex **6** which are not observed experimentally. At the same time, calculated and experimental geometries of complex **9** differ significantly in N2-C6-C7-C8 torsion angle due to participation of the CH_2OH group in hydrogen bonding with both N1-H1N group and acetone molecule. Therefore, weak influence of the crystal packing is observed for **6** (see Fig. S46), while it is much more pronounced in the case of **9**.

Table S3. Selected characteristics of molecular geometry of compounds **6** and **9** (torsion angles in deg. distances in Å). For calculated molecules, energies of nonbonded contacts (in kcal/mol) are given in brackets if the bond critical point was localized. [a]

Torsion angle or nonbonded contact	Complex **6** (X-ray)	Complex **6** (Calcd.)	Complex **9** (X-ray)	Complex **9** **(**Calcd.)
B8-N1-C3-C4	-176.9(2)	-177.2	-175.0(2)	179.8
B8-N1-C3-N2	-0.4(3)	-0.3	2.3(2)	-2.8
N1-C3-C4-C5	101.0(2)	91.9	97.7(2)	97.9
N1-C3-N2-C6	174.0(2)	177.7	-178.2(2)	175.2
C3-N2-C6-C7	136.9(2)	161.8	134.9(2)	135.3
N2-C6-C7-C8	-71.3(2)	-63.7	177.8(2)	-74.2
C6-C7-C8-O1	-	-	64.8(2)	-59.4
B4-H4…H2N-N2	1.94(4)	1.82 [-3.7]	1.89(4)	1.81 [-3.8]
C2A-H2A…N2	2.69(2)	2.57 [-1.6]	2.56(2)	2.56 [-1.6]
C2A-H2A…H8B-C8	2.26	2.32 [-1.0]	2.72	2.11 [-1.3]
B6A-H6C…H5C-C5	2.48	2.55 [-0.6]	2.49	2.59 [-0.5]
B4-H4…H8B-C8	3.62	2.44 [-0.8]	-	-
B7A-H7C…H8B-C8	3.93	2.70 [-0.5]	-	-
C5-H5B…O1	-	-	3.35(2)	2.38 [-1.8]

[a] for experimental structures, nonbonded distances are calculated using H-C(N,O,B) bond lengths normalized according to neutron diffraction studies (C-H, 1.09 Å; N-H, 1.01 Å; O-H, 0.96 Å, B-H, 1.18 Å). These distances nearly coincide with those from quantum chemical calculations. All results are given for symmetry independent part only.

Table S4. Selected characteristics of molecular geometry of compounds **18** and **19** (torsion angles in deg. distances in Å). For calculated molecules, energies of nonbonded contacts (in kcal/mol) are given in brackets if the bond critical point was localized. [a]

Torsion angle or nonbonded contact	Complex **19** (X-ray) *transoid*	Complex **19** (Calcd.) *transoid*	Complex **19** (Calcd.) *gauche*	Complex **18** (X-ray)
relative orientation of the ligands [b]	180	180	111.4	180
C1-B4-B8-O1	156.1(2)	156.5	157.5	157.2
B4-B8-O1-C3	179.1(2)	176.4	177.9	-179.3(2)
B4-B8-O1-C7	38.6(2)	34.9	35.7	41.7(3)
B8-O1-C3-C4	154.2(2)	156.4	156.1	158.2(2)
B8-O1-C7-C6	-154.7(2)	-156.4	156.2	-158.4(2)
C1A-H1A…H4A-C4	2.28	2.41 [-0.8]	–	2.45
C2A-H2A…H6A-C6	2.41	2.41 [-0.8]	2.47 [-0.7]	2.51
C1A-H1A…O1	2.69(2)	2.66	–	2.69(2)
C2A-H2A…O1	2.74(2)	2.66	2.69	2.68(2)
B7A-H7A…H4A-C4	–	–	2.33 [-1.2]	–
B7A-H7A…H7B-C7	–	–	2.31 [-1.4]	–
B7A-H7A…O1	–	–	2.78	–
Calculated total relative energy	–	3.8	0	–

[a] for experimental structures, non-bonded H-C(B) distances are given in the same way as in Table S1. Empty cells in the Table means that atom…atom distance is significantly longer than sum of van-der-Waals radii. For molecules with *transoid* conformation (which are centro-symmetrical), relative orientation of the substituents and system of noncovalent contacts are given for symmetry independent part only. Strictly speaking, calculated structure of **19** with *gauche* conformation is not symmetrical, however in both ligands relative orientation of the tetrahydropyran ring is the same, and given only once.

[b] pseudo torsional angle B8-center(C1-C2-B7-B8-B4)…center(C1A-C2A-B7A-B8A-B4A)-B8A is given to define relative orientation of the dicarbollide ligands.

Table S5. Selected characteristics of molecular geometry of compound **17** (torsion angles in deg. distances in Å). For calculated conformations, energies of nonbonded contacts (in kcal/mol) are given in brackets if the bond critical point was localized. [a]

Torsion angle or nonbonded contact	Complex **17** (X-ray) *gauche*	Complex **17** (Calcd.) *gauche*	Complex **17** (Calcd.) *transoid*
relative orientation of the ligands [b]	110.8(8)	105.3	180.0
C1-B4-B8-O1	159.6(4)	159.2	157.8
B4-B8-O1-C3	175.1(5)	178.7	179.7
B4-B8-O1-C6	32.9(7)	27.5	33.9
B8-O1-C3-C4	151.9(4)	179.6	171.0
B8-O1-C6-C5	-127.2(4)	-156.3	-145.5
C1A-B4A-B8A-O1A	159.2(4)	159.2	157.8
B4A-B8A-O1A-C3A	177.4(4)	178.7	179.7
B4A-B8A-O1A-C6A	29.5(7)	27.5	33.9
B8A-O1A-C3A-C4A	-141.8(4)	-156.2	-145.5
B8A-O1A-C6A-C5A	168.3(4)	179.6	171.0
B9-H9…H3A-C3	2.13	2.16 [-1.9]	2.17 [-1.8]
B12-H12…H6C-C6	2.26	2.28 [-1.6]	2.18 [-2.0]
C2A-H2A…H3B-C3	2.33	2.20 [-1.1]	2.23 [-1.1]
B7A-H7A…H6B-C6	2.43	2.02 [-1.9]	–
B9A-H9A…H3AA-C3A	2.26	2.16 [-1.9]	2.17 [-1.8]
B12A-H12A…H6CA-C6A	2.26	2.28 [-1.6]	2.18 [-2.0]
C2-H2…H3BA-C3A	2.26	2.20 [-1.1]	2.23 [-1.1]
B7-H7…H6BA-C6A	2.26	2.02 [-1.9]	–
C1A-H1A…H6B-C6	–	–	2.13 [-1.3]
C1-H1…H6BA-C6A	–	–	2.13 [-1.3]
C1A-H1A…O1	–	–	3.23
B7A-H7A…O1	2.80	2.73	–
C2A-H2A…O1	2.66	2.93	3.23
C1-H1…O1A	–	–	3.23
B7-H7…O1A	2.85	2.73	–
C2-H2…O1A	2.69	2.93	3.23

Calculated total relative energy		0	4.1

[a] for experimental structures, nonbonded H-C(B) distances are taken the same as in Table S1. Empty cells in the Table means that atom…atom distance is significantly longer than sum of van-der-Waals radii.

[b] relative orientation is defined as in Table S2.

Table S6. Selected characteristics of molecular geometry of compound **20** (torsion angles in deg. distances in Å). For calculated conformations, energies of nonbonded contacts (in kcal/mol) are given in brackets if the bond critical point was localized. [a]

Torsion angle or nonbonded contact	Complex **20** (X-ray)	Complex **20** (Calcd.) *gauche*	Complex **20** (Calcd.) *transoid*
relative orientation of the ligands [b]	104.8(9)	91.1	180
C1-B4-B8-O1	160.2(5)	159.3	159.5
B4-B8-O1-C3	178.7(5)	176.0	152.8
B4-B8-O1-C5	16.8(8)	17.3	16.0
B8-O1-C3-C4	-107.9(5)	-102.5	78.5
B8-O1-C5-C6	-138.5(5)	-141.4	-145.7
C1A-B4A-B8A-O1A	160.9(9)	159.3	159.5
B4A-B8A-O1A-C3A	-179.5(6)	176.0	152.8
B4A-B8A-O1A-C5A	20.3(9)	17.3	16.0
B8A-O1A-C3A-C4A	-106.9(5)	-102.5	78.5
B8A-O1A-C5A-C6A	-141.1(5)	-141.4	-145.7
B12-H12…H4B-C4	2.43	2.29 [-1.3]	–
C2A-H2A…H5C-C5	2.31	2.27 [-1.2]	–
C2A-H2A…H6B-C6	2.25	2.43 [-0.9]	–
B7A-H7A…H6B-C6	3.04	2.77 [-0.5]	–
B12A-H12A…H4AB-C4A	2.37	2.29 [-1.3]	–
C2-H2…H5AB-C5A	2.42	2.27 [-1.2]	–
C2-H2…H6AB-C6A	2.31	2.43 [-0.9]	–
B7-H7…H6AB-C6A	3.07	2.77 [-0.5]	–
C1A-H1A…H6B-C6	–	–	2.12 [-1.6]
C1A-H1A…H5B-C5	–	–	2.14 [-1.8]
C2A-H2A…H4B-C4	–	–	2.44 [-0.8]
B7-H7…H5B-C5	–	–	2.08 [-2.7]
B4-H4…H4C-C4	–	–	2.13 [-1.7]
B9-H9…H3B-C3	–	–	2.07 [-2.5]
C1A-H1A…O1	–	–	2.74
B7A-H7A…O1	2.68	2.62 [-1.9]	–
C2A-H2A…O1	2.78	3.01	271

C1-H1…O1A	–	–	2.74
B7-H7…O1A	2.67	2.62 [-1.9]	–
C2-H2…O1A	2.84	3.01	271
Total relative energy	–	0	6.3

[a] for experimental structures, nonbonded H-C(B) distances are taken the same as in Table 1. Empty cells in the Table means that atom…atom distance is significantly longer than sum of van-der-Waals radii. For calculated transoid conformation, the H…H intramolecular contacts are given only for symmetrically independent part

[b] relative orientaion is defined as in Table S2

Table S7. Values of H…LP-O angles for calculated and experimental structures of compounds **17**, **19** and **20**.

	19 (X-ray)	**19** (Calcd.)	**17** (X-ray)	**17** (Calcd.)	**20** (X-ray)	**20** (Calcd.)
H1A…LP-O1	130.7	130.8	–	–	–	–
H2A…LP-O1	136.3	130.8	127.5	126.6	121.5	118.9
H7A…LP-O1	–	–	127.0	137.1	138.8	147.9

[a] Because orientations of substituents for compounds **17** and **20** are nearly the same for both cages, the H…LP-O angles are given for one cage only.

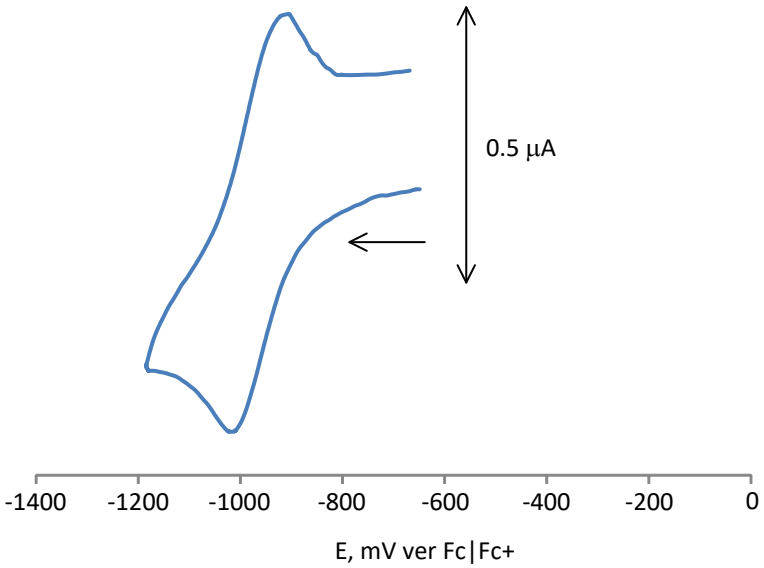

Figure S47. A CVA curve recorded at platinum disk electrode for [8,8'-$(EtO)_2$-3,3'-Fe(1,2-$C_2B_9H_{10})_2]^-$. Solvent - 1,2-dichloroethane with 0.2 M Bu_4NPF_6 (supporting electrolyte), T = 25°C.

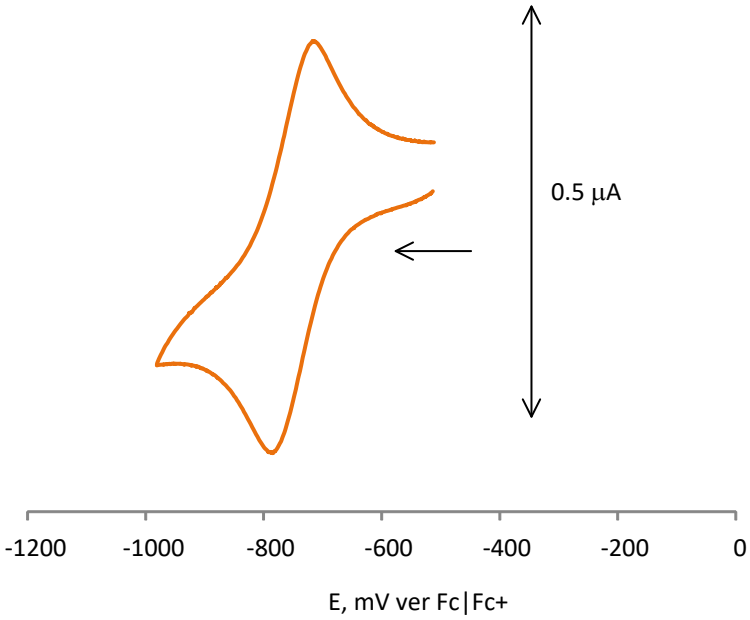

Figure S48. A CVA curve recorded at platinum disk electrode for [8,8'-$(MeS)_2$-3,3'-Fe(1,2-$C_2B_9H_{10})_2]^-$. Solvent - 1,2-dichloroethane with 0.2 M Bu_4NPF_6 (supporting electrolyte), T = 25°C.

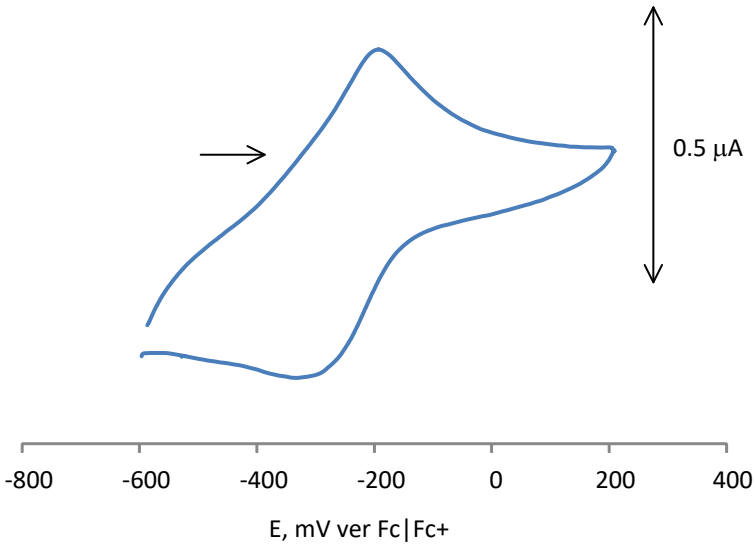

Figure S49. A CVA curve recorded at platinum disk electrode for [8,8'-($Me_2NCH_2CH_2NHC(Et)=HN)_2$-3,3'-Fe(1,2-$C_2B_9H_{10}$)] (**10**). Solvent - 1,2-dichloroethane with 0.2 M Bu_4NPF_6 (supporting electrolyte), T = 25°C.

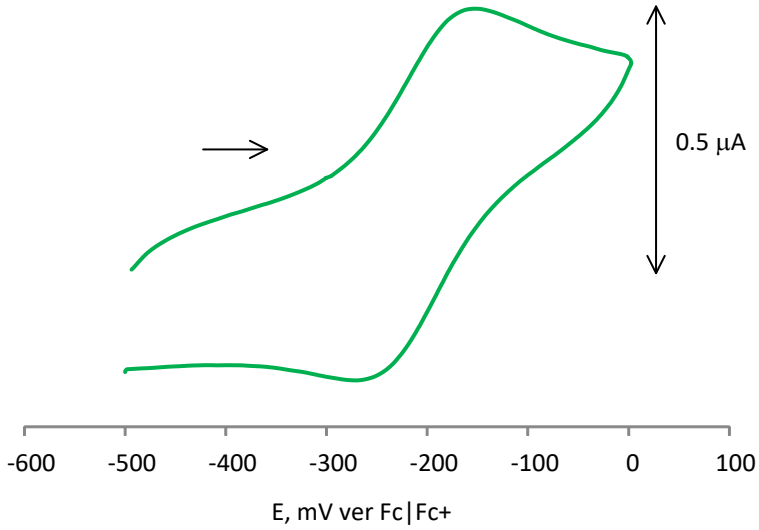

Figure S50. A CVA curve recorded at platinum disk electrode for [8,8'-($HOCH_2CH_2NHC(Et)=HN)_2$-3,3'-Fe(1,2-$C_2B_9H_{10}$)$_2$] (**8**). Solvent - 1,2-dichloroethane with 0.2 M Bu_4NPF_6 (supporting electrolyte), T = 25°C.

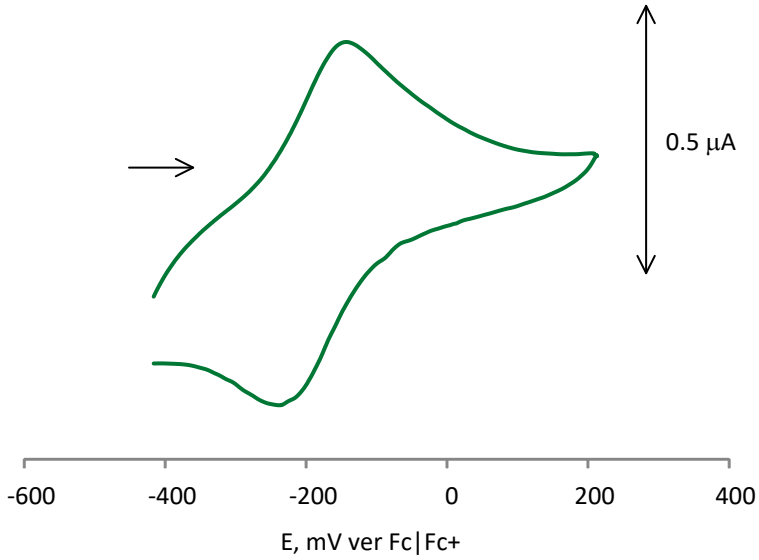

Figure S51. A CVA curve recorded at platinum disk electrode for [8,8'-($HOCH_2CH_2CH_2NHC(Et)=HN)_2$-3,3'-$Fe(1,2\text{-}C_2B_9H_{10})_2$] (**9**). Solvent - 1,2-dichloroethane with 0.2 M Bu_4NPF_6 (supporting electrolyte), T = 25°C.

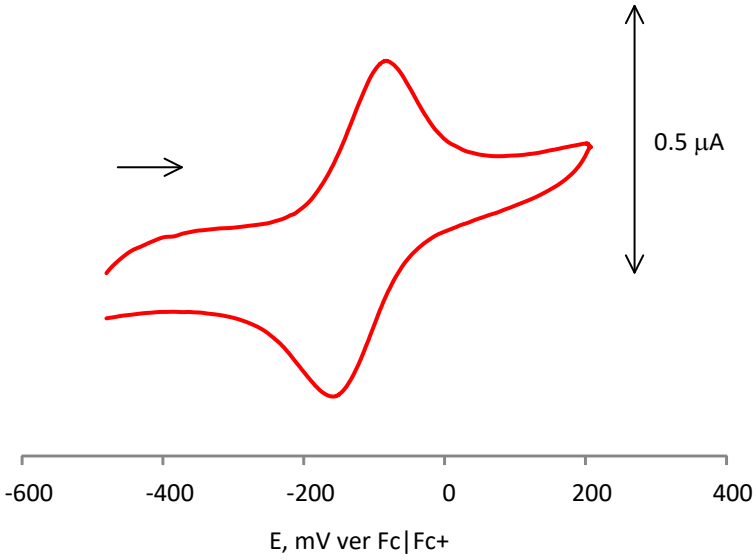

Figure S52. A CVA curve recorded at platinum disk electrode for [8,8'-($PhNHC(Et)=HN)_2$-3,3'-$Fe(1,2\text{-}C_2B_9H_{10})_2$] (**7**). Solvent - 1,2-dichloroethane with 0.2 M Bu_4NPF_6 (supporting electrolyte), T = 25°C.

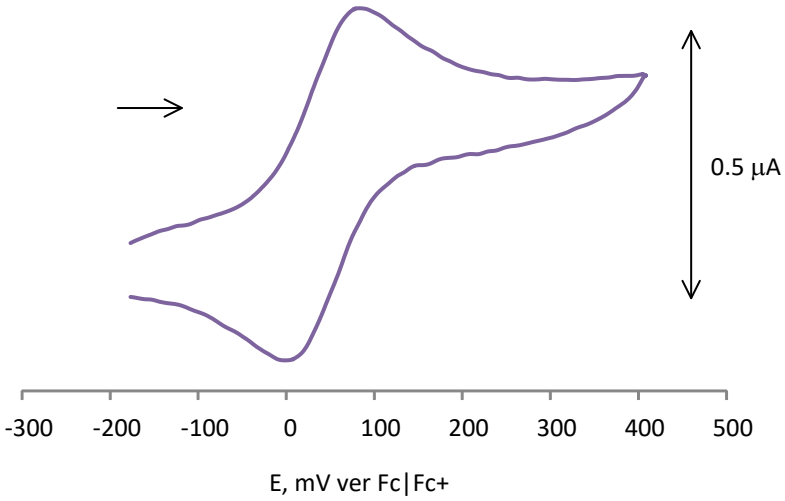

Figure S53. A CVA curve recorded at platinum disk electrode for [8,8'-((CH$_2$)$_5$O)$_2$-3,3'-Fe(1,2-C$_2$B$_9$H$_{10}$)$_2$] (**19**). Solvent - 1,2-dichloroethane with 0.2 M Bu$_4$NPF$_6$ (supporting electrolyte), T = 25°C.

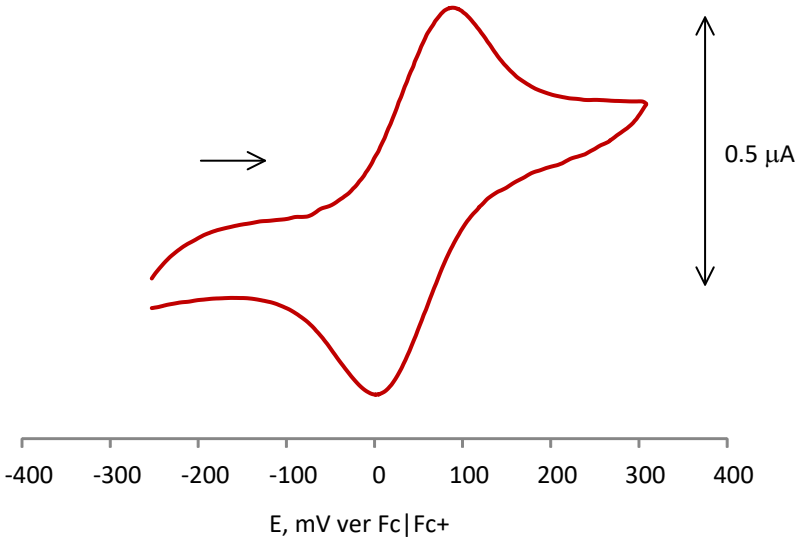

Figure S54. A CVA curve recorded at platinum disk electrode for [8,8'-(Et$_2$O)$_2$-3,3'-Fe(1,2-C$_2$B$_9$H$_{10}$)$_2$] (**20**). Solvent - 1,2-dichloroethane with 0.2 M Bu$_4$NPF$_6$ (supporting electrolyte), T = 25°C.